1

Engineering of Metal Active Sites in MOFs

Carmen Fernández-Conde, María Romero-Ángel, Ana Rubio-Gaspar, and Carlos Martí-Gastaldo

PhD Researchers on Functional Inorganic Materials Team (FuniMat), Instituto de Ciencia Molecular (ICMol) - Universidad de Valencia, C/ Catedràtic José Beltrán, 2, Vivero 1, 46980, Paterna, Spain

From their appearance, metal–organic frameworks (MOFs), have been an interesting field of research, partly due to the vast possibilities these materials offer [1]. The fact that they can be designed chemically to serve specific applications has already been proved in diverse areas such as gas separation [2], encapsulation [3] carbon capture [4], or catalysis [5–8].

Regarding catalysis, MOFs present many characteristics that make them potential candidates to carry out relevant catalytic processes as well as understanding the mechanisms through which these reactions take place. First of all, MOFs are heterogeneous catalysts, which can have an impact on separation, recyclability, and the possibility to operate in continuous mode, key aspects from an industrial standpoint. Additionally, heterogeneous catalysts often exhibit lower deactivation rates, compared to their homogeneous counterparts, mainly due to the spatial separation of the active sites avoiding its aggregation. However, there are some issues that limit the potential of traditional heterogeneous catalysts. In some cases, diffusion might prevent reagents from reaching the catalytic center, which is often poorly defined and understood. This lack of understanding also impacts the possibilities of modification of the catalyst, resulting in little room for improvement in these catalysts.

MOFs can serve as a platform for overcoming these drawbacks due to their inherent properties. Among the advantages of MOFs, it stands the isolation of the catalytic center and its uniform distribution along the framework, the sizeable porosity that enhances diffusion or the crystalline structure of these materials, which opens the door to the use of advance of characterization techniques. For all of this, research in MOFs as catalysts has become an attractive area. In this chapter, we will focus on metal-based catalysis in MOFs, which have already shown promising results in diverse catalytic processes. We intend to provide the reader with a general perspective of the different strategies used for engineering catalytic active sites in these porous, molecular frameworks. This chapter is divided into three different sections, attending to which component of the framework (metal node, organic

Catalysis in Confined Frameworks: Synthesis, Characterization, and Applications, First Edition.
Edited by Hermenegildo Garcia and Amarajothi Dhakshinamoorthy.

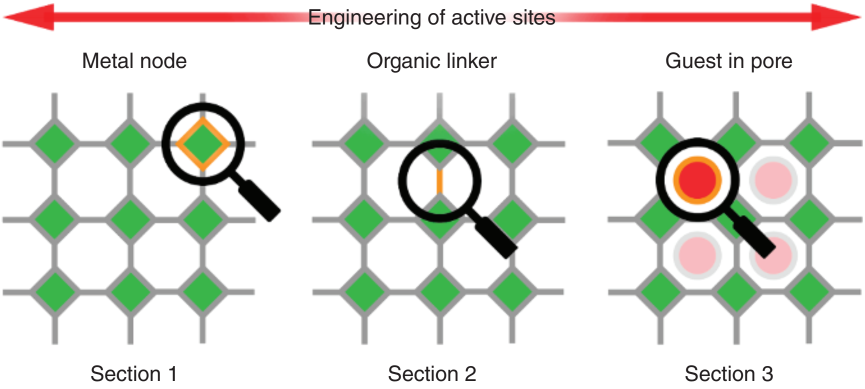

Figure 1.1 Schematic view of the three sections of this book chapter focused on engineering of active sites based on metal node, organic linker, or encapsulated guest. Source: Figure produced by the authors of the chapter.

linker, or guest) is responsible for the catalytic activity. Finally, different chemical incorporation strategies, characterization techniques, and examples of chemical reactivity of these reactive sites will be provided. This way, the structure of this chapter is shown in Figure 1.1.

1.1 Metal Node Engineering

This section will examine the different approaches used to obtain an active catalytic site in the nodes of MOFs, with the aim to be used in metal-based reactivity. Thus, this section of the chapter is divided into three main blocks, as represented in Figure 1.2. The first one comprises MOFs with intrinsically active metal nodes,

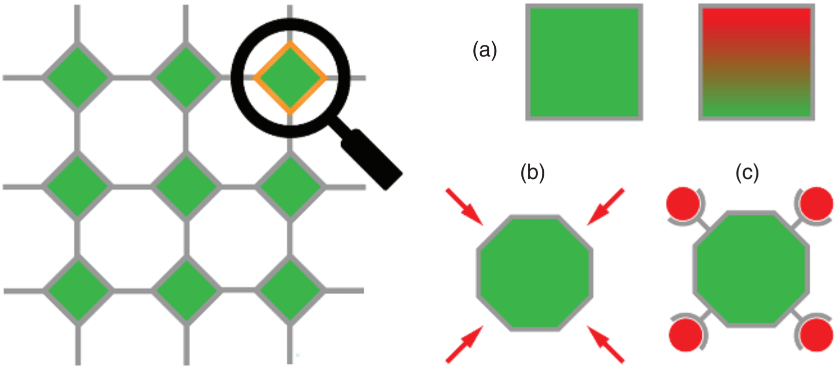

Figure 1.2 Schematic representation outlining the first section of the chapter: metal-based reactivity based on the engineering of the metallic cluster of MOFs through different strategies: intrinsic active metal sites with one or more than one metal (a), implantation of reactivity through the creation of defects (b), and incorporation of a metallic unit into the node cluster (c). Source: Figure produced by the authors of the chapter.

which can be further divided depending on the composition of the node. This way, this section will go through MOFs containing only one metal and MOFs with more than one (both mixed-metal and heterometallic MOFs).

The focus of the second part of the chapter deals with the introduction of defects as a way to increase the node performance in catalytic processes. Finally, the third part discusses different approaches that have been used to attach metallic units to the framework nodes. For each sub-section, we describe the different strategies used to tailor activity, the characterization techniques required for controlling and rationalizing activity, and different examples to illustrate their application in heterogeneous catalysis.

1.1.1 Frameworks with Intrinsically Active Metal Nodes

1.1.1.1 Metal–Organic Frameworks with Only One Metal

One of the main reasons why MOFs have attracted that much attention in recent years is their great chemical versatility. In fact, as this chapter explains, there are many ways to introduce specific functionalities to our frameworks, ultimately leading to better-performing materials. Here, we will turn our attention to the different kinds of homometallic clusters that can be found within MOFs, as well as their potential applicability in catalysis. In this part of the chapter, the use of MOFs containing only one metal, the so-called homometallic MOFs, and its application in the catalysis field will be briefly outlined.

In Figure 1.3, some of the most representative clusters are depicted, showing some of the extensive possibilities for constructing the framework. Being metallic nodes as extensive as they are, it is quite challenging to try to explain all their associated reactivity. In fact, MOFs, with certain kind of metals, are being used for redox and

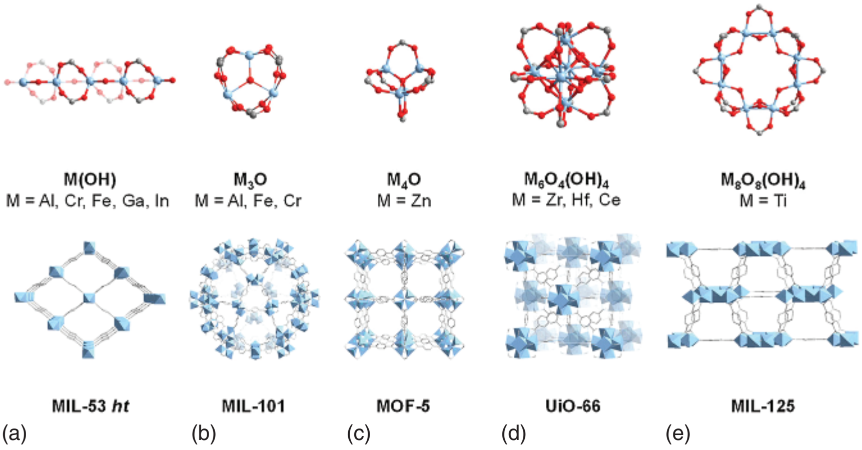

Figure 1.3 Representation of some of the most representative metal nodes that can be found (a) as well as the framework they form upon coordination with a binding organic ligand (b). Source: Reproduced with permission from Yang et al. [9]/American Chemical Society.

photocatalysis. Because of that, we will only consider the reactivity associated with Lewis and Bronsted-based catalysis.

In many cases, the reactivity of the metal cluster mainly comes from uncoordinated metal sites, the so-called open metal site (OMS). The catalytic power of these unsaturated centers is closely related to the Lewis acidity of the metal. This way, highly charged cations at the nodes, associated with high Lewis acidity, are good candidates for carrying out reactions based on Lewis acidity. In order to increase its reactivity, different activation processes can be applied to the pristine material. Furthermore, coordinated molecules can have Brønsted acidic character, as it has been proposed for adsorbed water in MOF-808-SO_4 [10].

Enhancing acidity-based reactivity in homometallic MOFs: creating open metal sites. Some post-synthetic treatments can be used to obtain a higher-performing catalyst and there exist different strategies that will be outlined here. The first one consists of a thermal reduction treatment to incorporate new OMS into MOFs as demonstrated by Serre et al. [11]. This strategy corresponds to Figure 1.4a which modifies the MIL-100(Fe) MOF. On the cluster of this framework, two of the terminal molecules coordinated to two Fe centers are water, while the third Fe can bear different molecules, mainly F- or OH-, depending on the synthetic conditions used to obtain it. The water molecules are easily removed, leaving two uncoordinated Fe centers at temperatures higher than 100 °C under vacuum or a gas stream. In their work, researchers demonstrated the possibility of thermally reducing the framework, appearing FeII OMS when heating the framework above 150 °C with a helium stream followed by 12 hours vacuum. Moreover, this work proved the relationship between unsaturated iron sites and the strength of

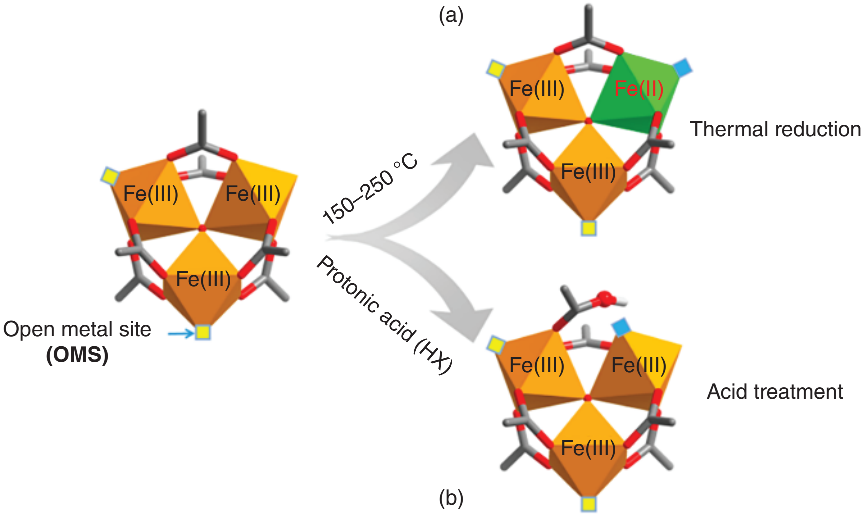

Figure 1.4 Schematic representation of the different proposed activation pathways by thermal reduction (a) and by the acid treatment (b). Source: Reproduced with permission from Wei et al. [12]/American Chemical Society.

interaction with gases, which has an impact on the performance of the framework for preferential gas sorption.

Another approach was followed by De Vos et al. [13] as a way to tune the catalytic properties of MIL-100(Fe). In this work, they treat the pristine framework with protonic acids, particularly CF3COOH and HClO4. The 1,3,5-benzenetricarboxylic acid, which serves as a ligand, is displaced from the cluster, resulting in the appearance of an OMS and an additional Brønsted acidic site, as represented in Figure 1.4b. In this case, a 2-fold increase in both Lewis and Brønsted acid sites after the acidic treatment of the framework is observed.

In other cases, the goal of the post-synthetic treatment might not be the creation of unsaturated sites within the node but maximizing the acidic character of a metal. This strategy was followed in the case of Lin et al. [14], who developed a synthetic procedure for designing a strongly Lewis acidic MOF. Particularly, they carried out a two-step transformation to the parent MOF-808 to obtain unsaturated Zr sites connected to triflate units, excellent withdrawing groups that maximize the Zr center's electron affinity, thus increasing its acidity.

Characterizing the active site in metal–organic frameworks. This part of the section will be centered on how to characterize the OMS introduced as well as the Brønsted acidity shown in the previous examples. Toward this goal, the use of probe molecules that interact differently with the different acidities present in the material has proven to be especially useful. This way, Fourier-transformed infrared spectroscopy (FTIR) spectra of adsorbed CO can give information on the formation of OMS and the presence of O-H stretching associated with Brønsted acidity [11, 13]. In the work of Lin et al. [14], in Figure 1.5, they could perform Density Functional Theory (DFT) studies to evaluate the most stable grafting mode of the triflate units. Additionally, in this case, Lewis acidity of the resulting material was quantified by N-methylacridone Fluorescence and compared with the pristine material, being an additional proof of the increased Lewis acidity.

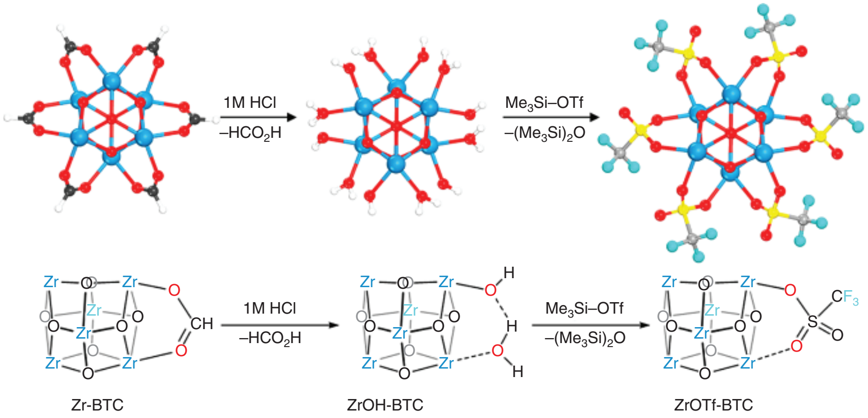

Figure 1.5 Synthetic procedure of the strongly acidic ZrOTf.BTC MOF through a two-step strategy. Source: Reproduced with permission from Ji et al. [14]/American Chemical Society.

Chemical reactivity in homometallic metal–organic frameworks. Acid catalysis has applications in many fields and is one of the most usual types. Amongst the reactions that can be used, the isomerization of a-pinene oxide [15], the cyclation of citronellal [16], the Friedel–Crafts acylation [17], or epoxide ring opening [18] reactions are common in the literature. Apart from its intrinsic value to synthetize certain products, the catalytic performance can be used to discriminate the different kinds of acidities found in a material, as exemplified by Corma et al. [19]

1.1.1.2 Metal–Organic Frameworks with more than One Metal in its Cluster

The thought of combining two or more metals in only one framework arises from the idea of having a material that combines their different characteristics of them. Bearing this in mind, ideally, these new materials can be useful to perform some applications in a more efficient way compared to homometallic MOFs. This combination of various metals can influence different applications such as gas sorption, catalysis, and sensing. Thus, for example, the incorporation of different metals (Mg/Ga, Mg/Fe, or Mg/V, among others) in the CPM-200s materials, showed an important effect on the CO_2 uptake capacity [20]. Also, the *doping* of the materials has also been studied [21, 22], demonstrating a clear effect on the electronic structure of the material, which is closely related to its performance in sensing and photovoltaic applications.

When it comes to catalysis, the use of a MOF with more than one metal results advantageous as both characteristics of these can be incorporated in one structure, which will be discussed later. However, for these MOFs having more than one metal, a distinction should be made according to the way these two or more metals are distributed in the structure. In fact, they can be statistically distributed along the framework, in which case, we would be talking *about mixed metal–organic frameworks* or, on the contrary, both metals are taking specific locations and are homogeneously distributed, then the term *heterometallic metal–organic framework* will be used. The achievement of this well-ordered disposition of metals is often restricted to the formation of clusters composed by more than one metal in specific proportions. The organization of the metals within the material structure can have a great impact on the catalytic performance of them. However, through the common characterisation techniques, it can be difficult to determine the metal distribution found in the material.

Mixed-metal or heterometallic MOF. In order to rationalize our catalytic findings and evaluate the effect of the distribution of metals in the material, one must be certain about it, often requiring specific characterization techniques. While some often-used analyses give information on the total amount of each metal, as it can be the case with inductively coupled plasma (ICP) or Energy-Dispersive X-Ray Spectroscopy (EDX) measurements, the need of exploring the exact positions of the metals usually requires more advanced techniques. In this way, the presence of domains or aggregates of one metal, which would prevent a homogeneous distribution, can be discarded.

Particularly, the heterometallic nature of clusters can be studied through Pair Distribution Function (PDF) analysis. There are many works devoted to an in-depth

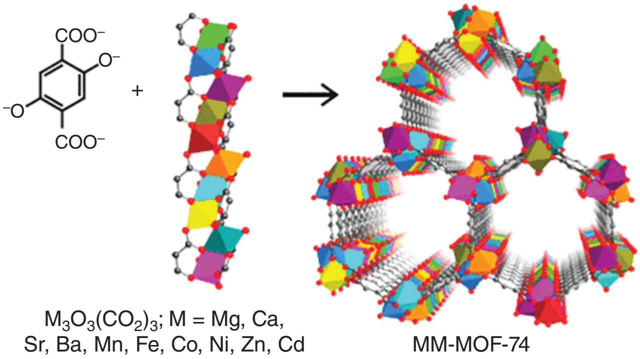

Figure 1.6 Representation of the family of mixed-metal MOF-74 showing all the metals that could be inserted in the structure. Source: Reproduced with permission from Wang et al. [27]/American Chemical Society.

analysis of this technique as well as its applicability to study different aspects of MOFs [23–25]. In summary, PDF analysis provides information about the distribution of distances between pairs of atoms from which information of the short-range order, or local structure of materials, can be extracted. As an example, PDF analysis was used in a work by Martí-Gastaldo et al. [26] to demonstrate the heterometallic nature of the cluster of a new family of MOFs.

Mixed-metal–organic frameworks. Most of the examples found in the literature for MOFs with more than one metal belong to the mixed-metal family. In this kind of materials, as previously explained, the metals are randomly distributed along the framework. One example of this is the work by Yaghi et al. [27] where they introduce different combinations of metals including Mg, Fe, Ni, or Co in the structure of MOF-74, obtaining the mixed-metal MOF-74, MM-MOF-74, schematically shown in Figure 1.6.

There are some other works involving mixed-metal MOFs [20, 28–30] and the influence of having the two metals has been evaluated in some aspects, such as flexibility [31, 32]. However, the influence of having two metals from a catalytic standpoint is still understudied, probably due to the difficulty of assessing the influence of each metallic center on the catalytic reaction.

Heterometallic Metal–Organic Frameworks. Heterometallic MOFs have been studied from different standpoints. Computationally, there have been studies shedding some light on the energetic stability and structural feasibility of different families of bimetallic heterometallic MOFs [30]. However, when it comes to the applications and advantages that heterometallic MOFs can offer, many works have failed to assess the difference that a particular distribution of metal can make. Instead, results are often presented without a direct comparison with homometallic materials, leaving aside the potential heterometallic materials can bring. However, some works demonstrate that this differentiation can be the source of radically different catalytic behaviors and should, by no means, be overlooked. Such is the case with the heterometallic MUV-101(Fe) [26], which is capable of degrading nerve agent

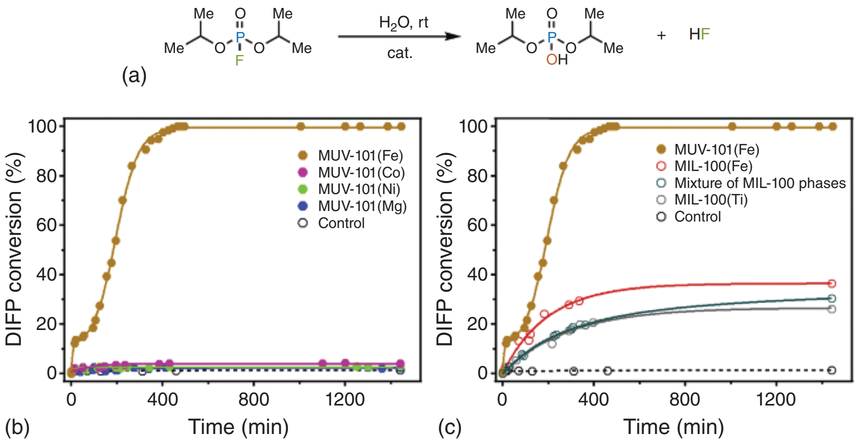

Figure 1.7 Different kinetic profiles for the degradation of a nerve simulant agent with heterometallic and homometallic MOF, as well as with the physical mixture of both. (a) Scheme of the hydrolytic degradation of DIFP, the chosen reaction to test the material reactivity in nerve agent degradation. (b) Hydrolysis profile of the different heterometallic titanium MOFs tested (c) Hydrolysis kinetics using heterometallic MUV-101(Fe), homometallic MIL(Fe) and MIL-100(Ti) and their physical mixture. Source: Reproduced with permission from Castells-Gil et al. [26]/Elsevier.

simulants, a function inaccessible for its isoreticular homometallic counterparts, MIL-100(Fe) [33], MIL-100(Ti) [34] and the physical mixture of both (Figure 1.7).

Another example, in which the exact disposition of the different metals contained in the MOF and its relationship with activity is studied, was presented by Deng et al. [35]. In their case, they could find that precoding the coordination number of heterometals in a MOF affected the electrochemical properties of MOFs, increasing its performance to carry out oxygen evolution reactions (OERs), as shown in Figure 1.8.

1.1.2 Introducing Defectivity as a Powerful Tool to Tune Metal-node Catalytic Properties in MOFs

The structure of MOFs, as many crystalline structures, often deviates from its ideal structure creating the so-called defects. These defects lead to changes in their mechanical and physical properties, porosity [36, 37], and density of OMSs. Ultimately, these defects can be somehow beneficial to the final application of the framework, tailoring its properties, for which a control and understanding of the defect engineering process is needed. Defect engineering of MOFs has already found applicability in gas storage [38, 39], or catalysis [13, 40], which will be the focus of this section.

Regarding defectivity, UiO family has been greatly studied due to its exceptional stability. In fact, the maintenance of this stability upon introduction of defects is probably the main reason why this family is often used as a model to exploit the defect engineering in MOFs. There are two basic classifications for defects in MOFs:

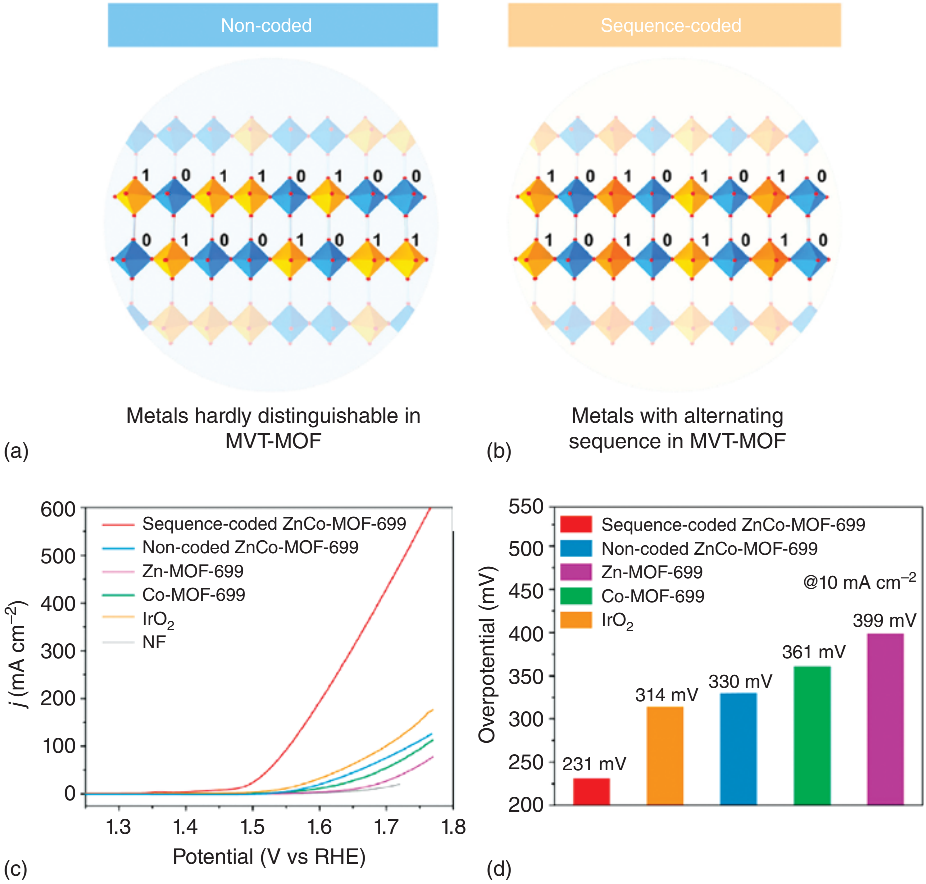

Figure 1.8 Representation of non-coded (a) and coded (b) MOFs and its electrochemical consequences: LSV (Linear sweep voltammetry) curves of different catalysts and electrodes in the OER test under the same conditions (c) and comparison of overpotentials (d). Source: Reproduced with permission from Jia et al. [35]/Elsevier.

the missing linker defects (MLD), or missing cluster defects (MCD), depending on the structural part involved in creating the defect, as illustrated in Figure 1.9 [41].

MLD originates from the loss of an organic linker from the framework while MCD is caused by the loss of the complete cluster. To compensate these vacant positions, different molecules can be incorporated the so-called caping ligands which include modulators, water molecules, or anions such as fluoride or chloride [42].

Chemical Incorporation. Briefly, the incorporation of defects to a MOF can be accomplished through two main strategies: *de novo* synthesis or by a post-synthetic treatment. The first one is the most widely used and relies on the addition of modulators to the reaction used to synthetize MOFs. Modulators are monocarboxylate species that connect to the metallic nodes as an organic linker would, but they only offer one-side connectivity, thus preventing two clusters from being connected. Typical modulator ligands include formic acid, acetic acid, trifluoroacetic acid, and

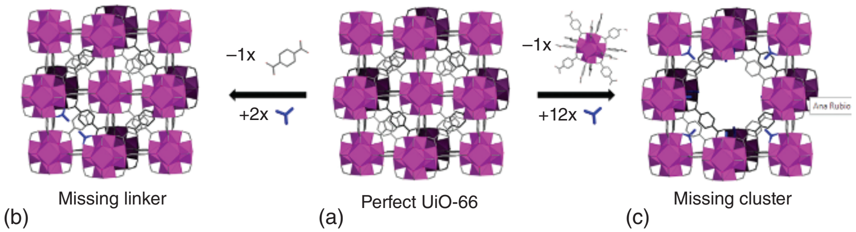

Figure 1.9 Schematic view of the generation of defects in UiO-66: from a perfect structure (a) to a missing-linker (b) and missing-cluster (c) defectivity. Source: Reproduced with permission from Taddei [41]/Elsevier.

difluoroacetic acid. It is beyond the scope of this chapter, but one should bear in mind that there are some factors influencing the creation of defects with modulators such as concentration, connectivity or acidity of them [42, 43].

When it comes to post-synthetic treatments to incorporate defectivity in MOFs, many methods rely on the acid/basic treatment of the pristine frameworks. Through this treatment, for example, defects were created in MIL-100(Fe) by the reprotonation of some 1,3,5-benzenetricarboxylic acid (BTC) linkers, removing them from the structure [13]. Additionally, monocarboxylate ligands can be incorporated into the structure in a Solvent-Assisted Ligand Incorporation fashion [44], where the framework is immersed in a solution containing the desired ligand.

Characterization Techniques. Many different techniques can be used to study the presence of defects in a MOF. One of the most used is Thermogravimetric Analysis (TGA), which provides an estimation of the number of defects present by comparing the theoretical weight loss of an ideal material with the real weight loss of the defective one. This can be correlated with the number of missing ligands per cluster, as reported by Lamberti et al. [45], shown in Figure 1.10.

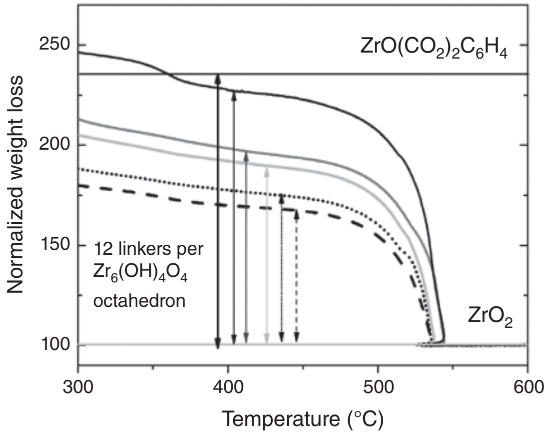

Figure 1.10 High-temperature part of the TGA curves for defective UiO-66 samples from which an estimation of the defects was made. Source: Reproduced with permission from Valenzano et al. [45]/American Chemical Society.

On other occasions, characterization techniques of the acid/base properties of a certain material can inform us about their defectivity. Thus, using probe molecules such as CO [13], pyridine [46], or CD_3CN [47], has been used to confirm the presence of defects as well as studying their newly introduced chemical properties.

X-ray diffraction patterns generally provide little information about defects. On the contrary, high-resolution neutron scattering has been employed to obtain evidence of the presence of caping ligands, proving missing linker defects [38].

Other techniques such as single-crystal X-ray diffraction, Extended X-Ray Absorption Fine Structure (EXAFS), or N_2 adsorption can also provide valuable information to study defective materials. However, with all the characterization techniques shown in this section, no information from the distribution of defects along the framework can be extracted. Recently, much effort has been dedicated to this issue, resulting in the development of a low-dose high-resolution electron microscopy (HRTEM) technique with electron crystallography [48]. The resultant images are shown in Figure 1.11 and show the types, distributions, and correlations as well as the exact three-dimensional structure of the defects in a UiO-66 framework.

Chemical Reactivity. The incorporation of defects can have a great impact on the catalytic properties of the MOF. Probably the most intuitive one could be related to enhancing diffusion inside the framework meaning that reactants can reach catalytic sites more easily. However, the chemistry of defective MOFs is different, and this can also be the cause of increased catalytic behavior. For example, MLD can become a new catalytic center through different pathways. It may be the case where the caping ligand is a solvent or formate/acetate molecule that may be removed upon activation, thus giving place to a Lewis acid site or, otherwise, the caping ligand may be a catalytic active specie, for example with Bronsted acidic character. Another option is to use these vacant sites to incorporate new ligands, with additional functionalities, or clusters to serve as catalytic centers, being this very similar to the topic that will be discussed in Section 1.2.2. These concepts are schematically illustrated in Figure 1.12 [42].

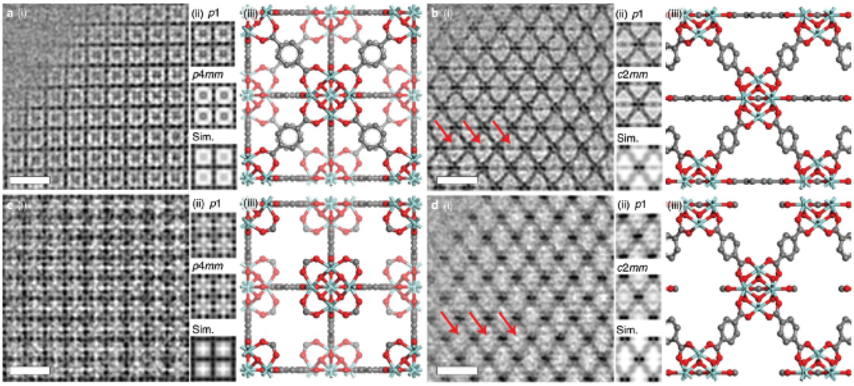

Figure 1.11 HRTEM analysis and structural models of perfect and missing-linker regions in defective UiO-66 along the [001] (a), [110] (b), [001] (c), and [110] (d) zone axes. Source: Reproduced with permission from Liu et al. [48], ©2019/Springer Nature.

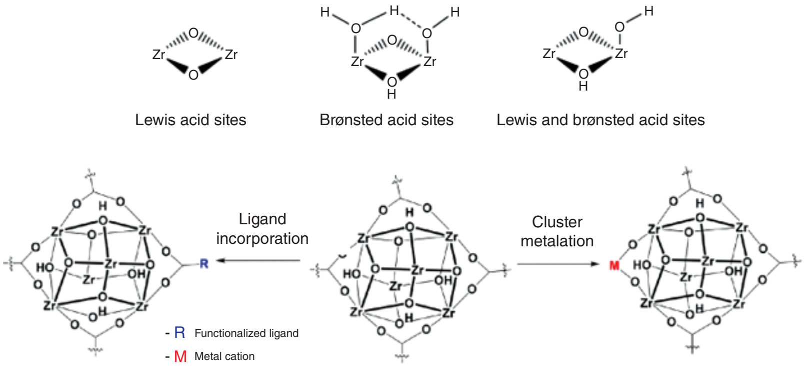

Figure 1.12 Illustration of the different types of reactivity associated with the engineering of defects and the possibilities to incorporate new catalytically active sites. Source: Adapted and reprinted with permission from Feng et al. [42]. Copyright 2021 American Chemical Society.

The enhanced reactivity as Lewis acids of defective MOFs has been exploited, for instance, in the citronellal cyclization reaction by the group of De Vos et al. [47]. In this work, the modulator approach with trifluoroacetic acid was followed in a UiO-66(Zr) MOFs, leading to a structure with a large number of OMSs upon activation.

The incorporation of defects can also provide the framework with more Brønsted acidic sites. This was exemplified by Farha et al. [40] in a study in which they correlate defects leading to inherent metal-bound hydroxides/water sites that can act as Brønsted acids with catalytic activity for the styrene oxide ring-opening reaction. In other cases, these metal-bound species can be displaced to incorporate reagents which would be impossible in the absence of defects. This strategy was used to carry out the hydrolysis of methylparaoxon [49], a phosphate-based nerve simulant upon displacement of water molecules connected to the nodes, as shown in Figure 1.13.

1.1.3 Incorporating Metals to Already-Synthetized Metal–Organic Frameworks: Isolating the Catalytic Site

In catalysis, the active site is often found on the atomic scale. For this reason, in order to maximize the material–reactivity relation, the more isolated our atoms can be, the higher the activity is expected compared to materials where atoms are aggregated. In fact, not only does aggregation prevent atoms from being exposed to the reaction media, thus inaccessible to reagents, but it can also deactivate them [50], as previously seen in the introduction of the chapter. Due to these, the use of single-metal-sites [51, 52] in catalysis has become really attractive, as it would contribute to overcoming these issues and MOFs are ideal candidates to incarnate them.

However, the introduction of some metals that might be interesting from a catalytic standpoint in MOFs by direct synthesis can sometimes prove challenging

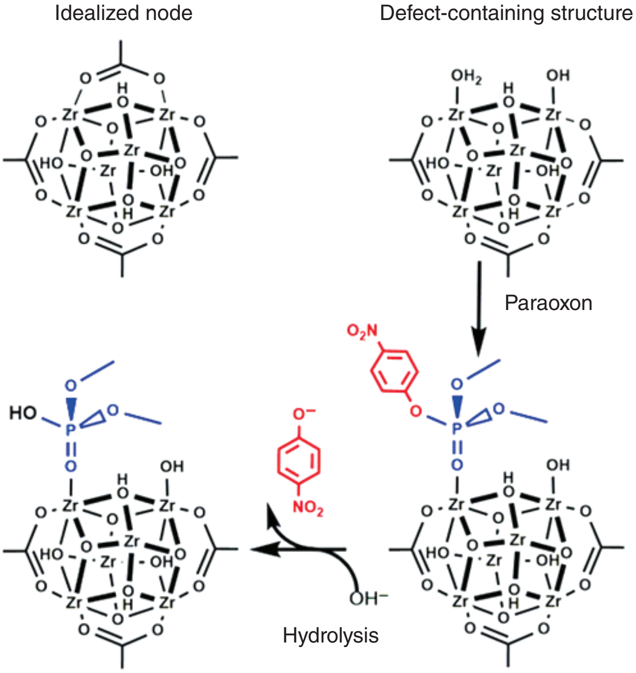

Figure 1.13 Representation of the reactivity enabled by missing-linker defectivity in UiO-66: coordination of the substrate into the node and subsequent attack of hydroxy anions. Source: Adapted and reprinted 49 from Yang et al. [9]. Copyright 2015 American Chemical Society.

This is due to the low solubility of its precursors, their high tendency to form oxides or several phases, or the low crystallinity of the resultant material. As a way to overcome this, new metals can be incorporated into an already-formed framework (*a posteriori*) through post-synthetic treatments [53].

Traditionally, the grafting of different metal species to a material has been done in diverse materials such as alumina, zirconia, or silica [54], often relying on the presence of –OH pending groups. Despite its great importance, however, the exact knowledge of the nature of the catalytic site still remains diffuse for many of the solids cited above. Furthermore, at other times, the leaching of these active species out of the support prevents its usefulness.

Recently, MOFs have been proposed as platforms to carry out this metal insertion and serving some of the already-commented advantages of MOFs (chemical versatility, sizable pores, high porosity). In this way, single-metal sites could be incorporated to MOFs.

Moreover, the incorporation of metals into MOFs offers additional advantages: these materials' crystalline structure can open the door to many techniques that would ultimately shed some light on the relationship between structure and activity as well as the mechanism through which the reaction takes place. Therefore, this finally paves the way toward a rational catalyst design. In this section, we will be turning our attention to how new metals can be incorporated to MOFs clusters and its advantages regarding catalysis.

Chemical incorporation: synthesizing MOFs with more than one metal. The incorporation of metallic units to the nodes of the framework post-synthetically can be divided into two big groups depending on whether a metal in the cluster is exchanged or, otherwise, an additional metal is incorporated to the metal node.

1.1.4 Metal Exchange

Chemical incorporation through metal exchange can be a method to integrate metals in the node that could not have been introduced by means of direct synthesis. This methodology is based on soaking of crystals in a solution where the metal is dissolved. This methodology was used in a work by Dinca et al. [55], in which they obtain MOF-5 with a great variety of metals, including reduced metal cations which are rare in MOF chemistry, mainly due to incompatibility of their oxidation states with the material synthetic conditions. The metals that were successfully incorporated in these MOFs are shown in Figure 1.14.

1.1.5 Attaching Metallic Units to the MOF

Over the years, two main strategies have been used to incorporate these metallic units into the framework: *Atomic Layer deposition (ALD)in MOFs (AIM)* or *Solvothermal deposition in MOFs (SIM)*, depending on the media that metalation takes place. Atomic layer deposition is a subclass of the chemical vapor deposition technique, in which "the precursor molecules deposit only at chemically reactive surface sites, being these reactions self-limiting" [56]. ALD is used for the "atomic-scale deposition of films on the surface of a chosen substrate" [57]. These ultra-thin films can be applied to different fields from which semiconductors stand out [58], where an exact control of homogeneity is crucial (Figure 1.15).

When applying ALD to MOFs, in AIM processes, some prerequisites have to be met: mesoporosity, thermal, and hydrolytic stability as well as functional groups to graft the metal in the correct disposition. The first example of AIM was carried out by Farha and co-workers [56] using NU-1000 as platform. This material had to be pretreated with HCl/DMF to remove the benzoic acid units initially coordinated to the pore and substitute them with -OH units, capable of carrying out metalation. Experimentally, the MOF powder was placed inside an ALD reactor with the metal

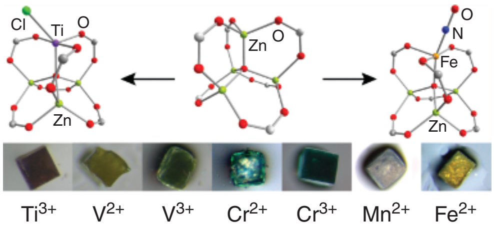

Figure 1.14 Illustration of all the possible metallic cations that can be introduced in the cluster of MOF-5 by using the metal exchange strategy. Source: Reproduced with permission from Brozek and Dincă [55], ©2013/American Chemical Society.

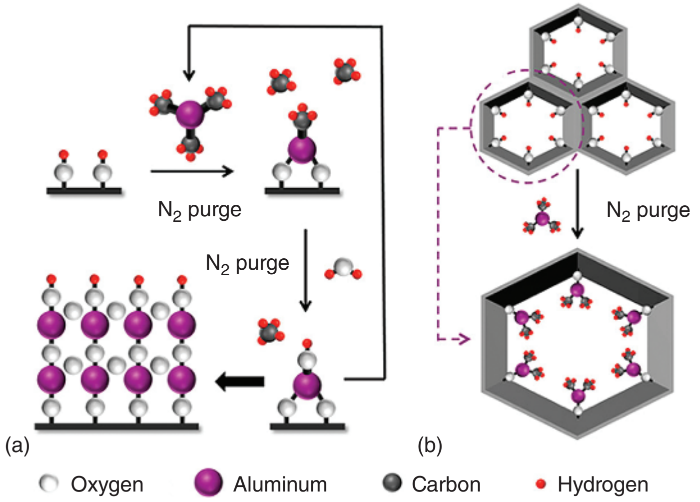

Figure 1.15 Illustration of the film ALD deposition on a surface (a) and the metalation by ALD in a MOF (AIM) (b). Source: Reproduced with permission from Mondloch et al. [56]/American Chemical Society.

salt submitted to temperatures around 120–150°C. After some exposure time, there is a N_2 purge to remove unreacted metal precursors.

In the case of solvothermal deposition in MOFs, the metalation takes place through the condensed phase. The experimental process is quite similar to AIM, being the metal precursor added in solution to the activated MOF, all in a non-coordinating solvent. Afterward, some washing is done to remove ungrafted metals [59]. It is important to highlight here that, in many cases, dry conditions are needed to carry out a successful grafting through SIM [60] (Figure 1.16).

Characterization Techniques of AIM and SIM. The insertion of different metals into the nodes of a MOF can be characterized in different ways. An interesting approach to check that the grafting has taken place is to study the FTIR -OH

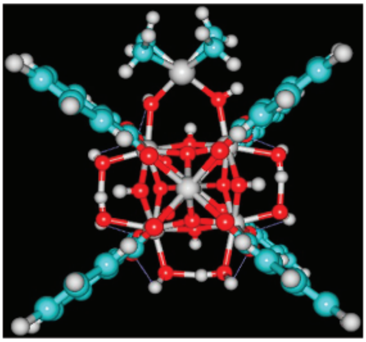

Figure 1.16 Representation of the grafting of Ir to the Zr_6 clusters of UiO-66. Source: Reproduced with permission from Yang et al. [59]/American Chemical Society.

or -OH_2 vibration bands which should diminish or disappear upon metal grafting. This was observed by Gates et al. [49] in their work on grafting of $Ir(CO)_2$ complexes in UiO-66 and NU-100 MOFs [59]. Complementarily, the number of metals inserted can be studied through inductively coupled plasma-mass spectrometry (ICP-MS) and give an estimated number of grafted metals per node.

X-ray absorption spectroscopy (XAS) and PDF studies can be really useful to gain some insight into the local structure of the supported metals. As an example, X-Ray Absorption Near Edge Structure (XANES) and EXAFS were used to support the grafting of Mo into NU-1000 [60] to be monomeric or at most few Mo atom clusters. In other cases, such as in the work from where Figure 1.17 is extracted [61], PDF is used to study the metal grafting mode to the cluster.

DFTs are also very important studies in assessing the accessible coordination modes of the metal [60, 61] and the energy it would take to interchange between them if it applies. Moreover, DFT studies might suggest the mechanism through which the catalytic reaction occurs through the new grafted material, as is the case of a Zn/Cu grafted NU-1000 MOF used for the selective hydrogenation of propyne [62].

Chemical Reactivity. This methodology allows the incorporation of chemical reactivity to the material that can be as diverse as the metals grafted. This way, many different reactions have been proposed for exploiting these chemically engineering metal sites in MOFs. Especially interesting are the cases where non-abundant metals are integrated in MOFs because their catalytic activity can be maximized with only a small amount of metal needed.

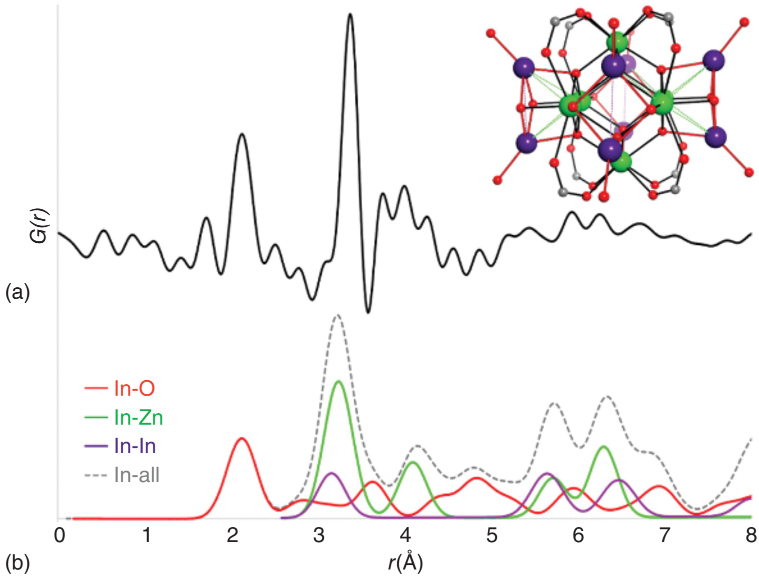

Figure 1.17 Differential PDF corresponding to the new atom–atom distances formed upon the incorporation of the In unit in the MOF through AIM methodologies (a), partial pair PDFs calculated based on the model for In-loaded NU-1000 structure predicted by DFT (b). Source: Reproduced with permission from Kim et al. [61]/American Chemical Society.

One of these examples could be the incorporation of a Molybdenum (VI) oxide catalyst in the clusters of a MOF via solvothermal deposition (SIM) [60]. With this material, the epoxidation of cyclohexene could be carried out selectively, being the epoxide and the ring-opened diol the main products. It is important to highlight that these oxomolybdenum species are active in homogeneous catalysis for the synthesis of epoxides but suffer from deactivation easily. In the past, these oxides have already been grafted to silica and alumina but, in these cases, there was evidence of considerable leaching. However, with the introduction of these Mo species into MOFs, this leaching seems to be suppressed, as the Hot-Filtration Tests carried out suggest, which is shown in Figure 1.18b.

Another example of catalyst based, but this time on AIM, was presented by Delferro et al. [52]. They grafted different metallic species to the node of NU-1000 and observed distinct reactivities depending on the metal grafted. While Zn afforded the isomerization of the product, Cu yielded a selective hydrogenation, as shown in Figure 1.19 [62].

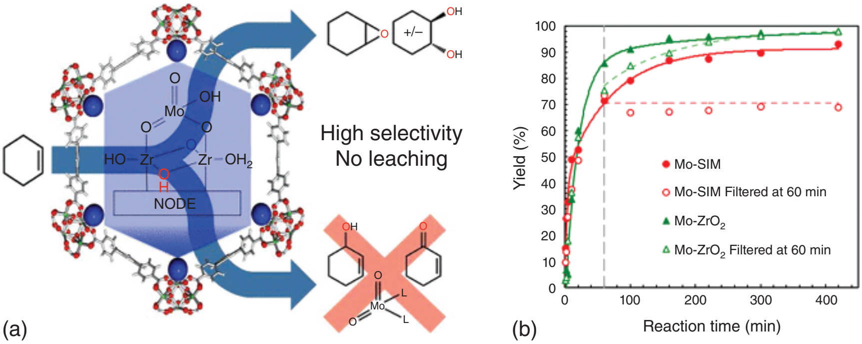

Figure 1.18 Illustration of the grafting of Mo species into the node and its consequences from a catalytic standpoint (a) and Hot-Filtration Tests used to discard the leaching of Mo into the reaction media (b). Source: Reproduced with permission from Noh et al. [60]/American Chemical Society.

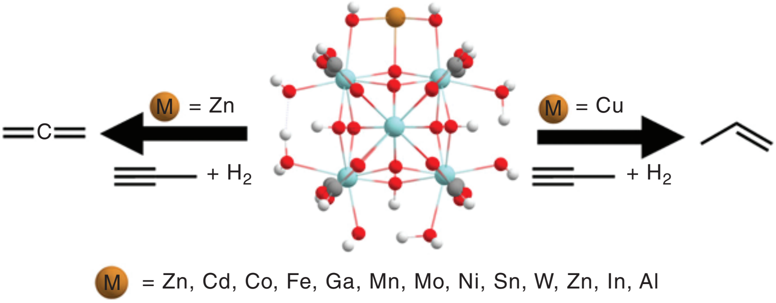

Figure 1.19 Illustration of the different reactivities enabled by the grafting of different metals to the metal–organic framework cluster. Source: Reproduced with permission from Hackler et al. [62]/American Chemical Society.

1.1.6 Grafting of Organometallic Complexes into the MOF Nodes

Since the appearance of organometallic chemistry, their advantages have been clear as these compounds allow a well-defined metallic catalytic site, which makes them highly efficient for catalytic processes as well as establishing structure-activity relations. Therefore, they have been proposed to catalyze industrially relevant processes such as the synthesis of polyethylenes with the organometallic Ziegler–Natta complexes. However, this type of compound usually operates in a homogeneous catalytic way fashion, which presents disadvantages in its practical use. On the view of having both, advantages of organometallic compounds (well-defined single site) and heterogeneous catalyst (easy separation and recyclability), researchers have worked toward the heterogenization of these by grafting them to solid supports thus getting the best of both worlds, being Jean Marie Basset one of the pioneers in the area.

Lots of effort has been put into trying to incorporate these organometallic compounds to the frameworks and can be carried out through different strategies, such as:

- Grafting the organometallic complex to the node.
- Inserting the organometallic compound through the ligand (Section 1.2 of this chapter).

At this point, it is worth mentioning that some grafted compounds can have different kind of ligands in their coordination sphere. In some cases, these ligands are one of those commonly used in organometallic chemistry, while other times these ligands are purely inorganic compounds such as hydroxides. In this direction, it is sometimes difficult to draw a line between the grafting of metals (that were covered in Section 1.2.2) and organometallic species. An example where different kind of ligands are coordinated to a metal grafted to a MOF-node is present in the work by Morsali et al. [63] as shown in Figure 1.20.

Chemical Incorporation of Organometallic Compounds to MOFs. One powerful approach to incorporate organometallic complexes to MOFs is through Surface Organometallic Chemistry (SOMC) [64, 65], which considers that the surface of the support can act as a ligand. In this way, grafting the metal complex to the surface of the MOF which ideally has a known structure and a specific chemical reactivity associated.

Traditionally, this SOMC approach has already been implemented in silica, alumina, and magnesia where –OH groups usually serve as anchoring points [66]. However, due to the advantages that MOFs can offer, great effort has been put to try to incorporate this SOMC approach to them.

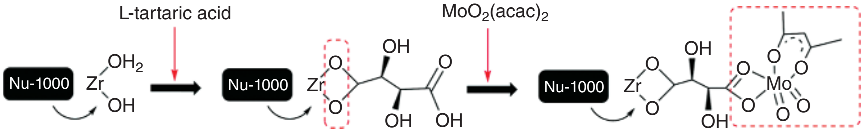

Figure 1.20 Insertion of L-tartaric acid and subsequently grafting with Mo.
Source: Adapted and reprinted with permission from Berijani et al. [63]. Copyright 2011 Royal Society of Chemistry.

Different metals can be incorporated to the clusters to obtain the desired reactivity. Usually, the chemical incorporation of them consists of the addition of the organometallic complex (itself or dissolved in an organic solvent) to the previously activated framework. Afterward, it is common that the material is washed with organic solvents and evacuated to eliminate any unreacted species.

There are many examples of different organometallic compounds being grafted to MOFs' nodes. Lin et al. [67] reported the insertion of an isolated magnesium alkyl catalyst connected through the metalation of $Zr_3(\mu_3\text{-OH})$ sites in the Secondary Building Unit (SBU) of the MOF. Another beautiful example is presented by Eddaoudi, Basset et al. [68] in a work in which, through a SOMC approach, a tungsten compound is grafted in a Zr-NU-1000 compound (Figure 1.21).

Characterization Techniques of Organometallic compounds in MOFs. As previously seen in previous sections, some commonly used techniques can apply to the characterization of these grafted organometallic compounds. Thus, while ICP-MS and EDX can quantify the metals incorporated, SEM-EDX mapping can assess its distribution. NMR techniques can be especially useful in this case, as they can be used to study if the ligand is still present and coordinated to the metal [68]. Moreover, FT-IR can give valuable information regarding the decrease of the Zr-OH band and the appearance of a M-ligand band upon grafting.

These modified frameworks can also be studied by means of single crystal X-ray diffraction, from which a complete vision of how the newly grafted organic compound is positioned with respect to the MOF can be extracted [50].

Computational studies can also be used to explore the more favorable grafting mechanism, taking into account that, as in many organometallic processes, many grafting scenarios could be possible.

Chemical Reactivity of Organometallic Compounds in MOFs. As seen in the last section, AIM and SIM reactivity depends mainly on the metal inserted giving rise to varied catalytic applications. It is also the case for the reactivity of organometallic compounds grafted to metallic clusters: the reactivity is so varied that we will only give a few examples of works published in the area. In fact, as we commented before,

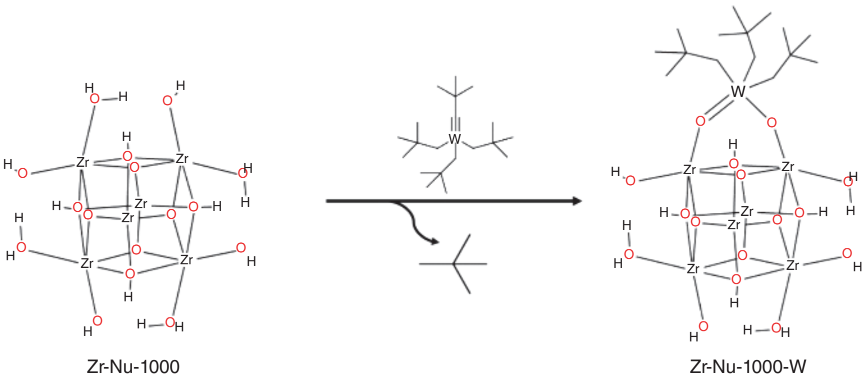

Figure 1.21 Grafting of a tungsten specie into the Zr nodes of NU-1000. Source: Adapted and reprinted with permission from Thiam et al. [68]. Copyright 2020 American Chemical Society.

the whole idea behind this post-synthetic treatment is to incorporate the same chemical reactivity found in organometallic chemistry to MOFs.

In this way, the strategy of SOMC has been applied to MOFs resulting in systems with higher catalytic turnover when compared to other catalysts based on the same metal. This is the case of the W complex grafted presented in the previously mentioned work by Basset and Eddaoudi et al. [68], showing better performances than other W-based catalysts. Particularly, this catalyst could be activated in the presence of an olefin, rendering an active carbene specie, active in the metathesis of olefins with good selectivity toward the primary products.

This example is of especial interest as it shows the potential advantages of this strategy. Apart from obtaining a competitive heterogeneous catalyst, the grafting mechanism and the actual structure of the precatalyst grafted W complex could be studied computationally, as shown in Figure 1.22. A deeper understanding of how this catalyst works could be obtained through this, and ultimately, improve the efficiency of industrial processes based on WO_3/SiO_3, where there is currently a lack of understanding.

Another example is the research carried out by Lin et al. [67]. In this case, the supported specie was a magnesium-alkyl which served as a catalyst in hydroboration and hydroamination reactions. This catalyst was demonstrated to be effective in hydroboration reactions with such low loadings as 0.05 mol% Mg and suitable to diverse substrates. Moreover, its recyclability and crystallinity maintenance were examined with excellent results. Although the position of the Mg grafted could not

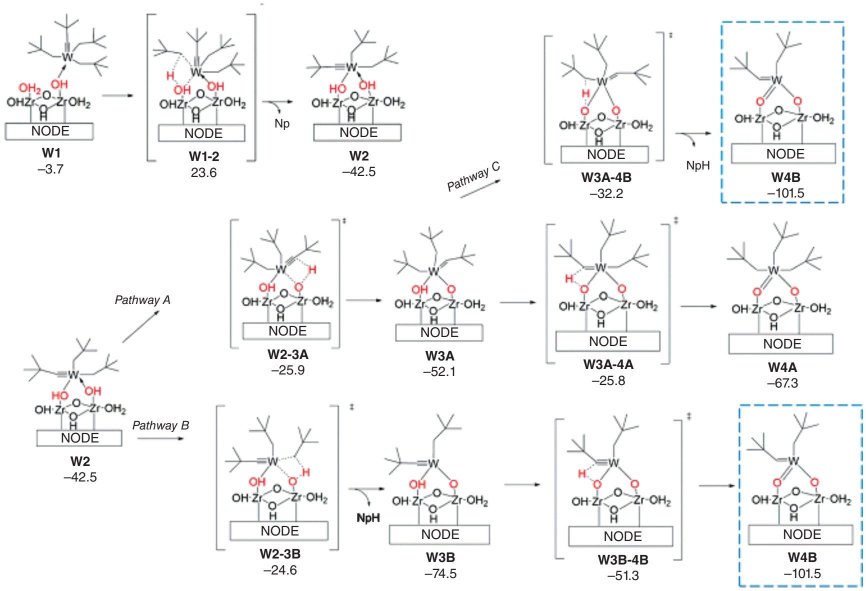

Figure 1.22 Grafting of the W-species to the node and the energy differences in kcal/mol calculated by DFT. Source: Reprinted with permission from Thiam et al. [68]. Copyright 2020 American Chemical Society.

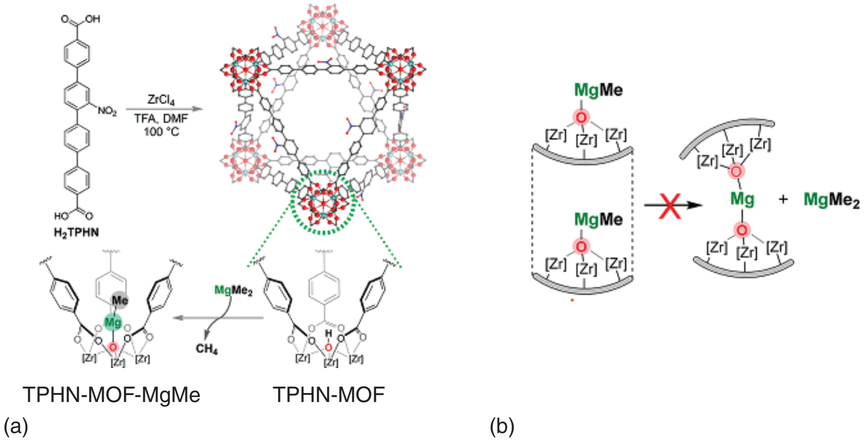

Figure 1.23 Synthesis of the TPHN-MOF and subsequent grafting in the metallic nodes of the structure of an alky-magnesium unit, THPN-MOF-MgMe (a) and benefits regarding the isolation of the active site within the framework ultimately preventing Schlenk-type ligand redistribution reactions (b). Source: Adapted and reprinted with permission from Manna et al. [67]. Copyright 2016 American Chemical Society.

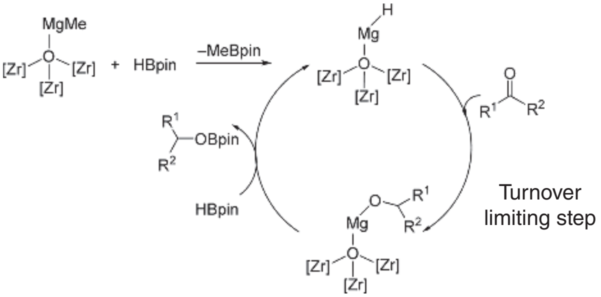

Figure 1.24 Proposed catalytic cycled of the organometallic Mg-grafted inserted into TPHN-MOF. Source: Adapted and reprinted with permission Manna et al. [67].

be determined by single-crystal diffraction due to disorder, the researchers proposed the structure shown in Figure 1.23.

All of this enabled the proposal of a tentative mechanism for the TPHN-MOF-Mg catalyzing hydroboration reactions, shown in Figure 1.24. In particular, they attributed the catalytic activity of the catalyst to the Mg atom, capable of activating the aldehyde unit.

1.2 Ligand Engineering

Through the last few years, researchers have made a lot of efforts to enhance the catalytic properties of MOFs [69–73]. One way to do that is by introducing a catalytic metal site, or several, into the structure [74]. This or these catalytic metal sites can

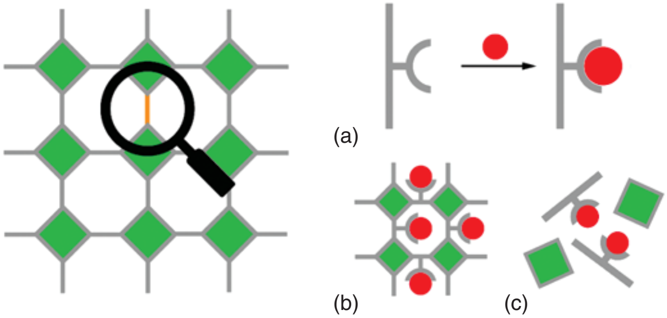

Figure 1.25 Schematic representation of the different linker metalation procedures: premetalation of the ligand (a), post-synthetic metalation (b), and introduction of the metal by direct synthesis (c). Source: Figure produced by the authors of the chapter.

be present in different parts of the framework, such as in the metal cluster [75], in the organic ligands [76], attached to the pores [77], or randomly distributed along the assembly [78], as mentioned in the introduction.

The grafting of diverse catalysts into the organic parts of the MOFs opens a new avenue for catalysis. As it is well known and studied, homogeneous and heterogeneous catalysts incorporated or embedded into the frameworks can give rise to more efficient catalytic processes, and particularly, MOF catalysts with active sites at organic linkers have attracted the attention in the last few years.

As it will be more detailed next, this part of the chapter will consist of the introduction of metal sites in the organic ligands of the MOF. Here, it will be described the different strategies to introduce the active metal sites into the organic parts of the framework, the variety of organic ligands that can be modified for that task, and the role of themselves in the catalytic process (Figure 1.25).

1.2.1 Ligands as Active Metal Sites

1.2.1.1 Creating Metal Sites in the Organic Linkers. Types of Ligands

Conceiving ligands as active sites for catalytic reactions is a well-studied area in the field of MOFs [79, 80]. MOFs are excellent platforms used in heterogeneous catalysis due to their tunability of the pore sizes, their high activity, and selectivity [81, 82]. Their organic part, the ligands, can also be modified by introducing different substituents like, for example, metal complex-based catalytic species which will improve the structural stabilization of the catalytic sites, create synergistic environments, or help in the interaction with substrates. Therefore, catalytic efficiency and selectivity are enhanced [83]. Introducing active metal moieties in the ligands is an easier technique than others used for the incorporation of metal nodes in MOFs, especially if it is done by post-synthetic modifications (PSM). But this can be achieved by both, direct synthesis and PSM. The insertion of single-metal sites in the ligand can be done before, after, or during MOF synthesis via coordination with their heteroatoms owning to lone pairs of electrons [84]. Direct methods are challenging due to the possible deactivation of the induced OMSs while introducing the metals, but on the contrary, as mentioned before, PSM are a more respectful, easier, and safer approach to generate highly catalytic active sites in the ligands after the MOF synthesis. This approach also includes the grafting of inorganic metal species or complexes onto the organic ligands and the exchange of metallolinkers.

Moreover, in MOFs with one metal in the structure acting as a catalytic single metal site, it is possible to include additional metals in some specific linkers denoted as metalloligands. These ligands are mainly constituted by N-donor atoms such as porphyrins [85], bipyridines [86], terpyridines [87], imines [88], salen [89], or diketiminates [90]. In this way, many homogeneous metal complexes that have catalytic active sites established can be attached to the metalloligands and provide various heterogeneous catalysts sites in the MOF that can work at the same time or not. This offers a bridge between heterogeneous and homogeneous catalysis that integrates their respective advantages into the MOF (Figure 1.26).

The first part of this chapter will be focused on the description of some examples of these kind of ligands that are the most commonly used for catalysis and how they are used for it. It is also described how they can interact with other single-metal sites that can be present in the MOF.

Porphyrin ligands. "Porphyrins are [18π]-electron heteroaromatic compounds in which the aromatic character of the underlying tetrapyrrole moiety, and the reactivity of the functional groups present in their side chains, governs their rich chemistry." [92]

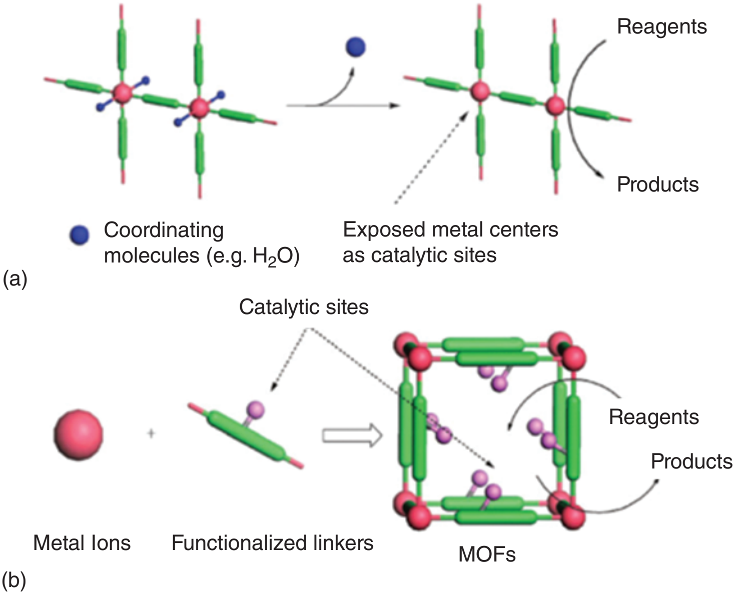

Figure 1.26 Illustration of the incorporation of active metal sites in MOFs: coordinatively unsaturated metallic nodes serving as catalytic sites (a) and incorporation of active catalytic sites into the ligands of MOFs (b). Source: Reproduced with permission from Ma et al. [91]/Royal Society of Chemistry.

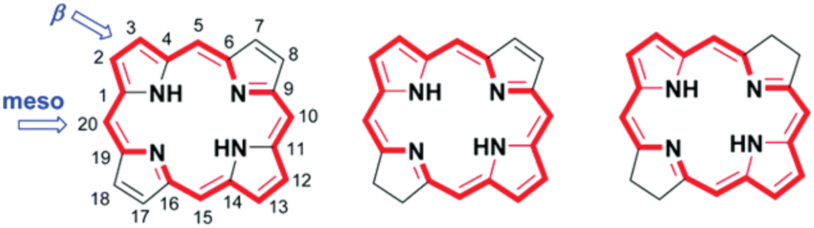

Porphyrin Chlorin Bacteriochlorin

Corrin Isobacteriochlorin

Figure 1.27 The different classification of macrocycles and their coordinative positions. Source: Reproduced with permission from Senge et al. [92]/Royal Society of Chemistry.

As Senge et al. commented in their review, porphyrins are organic compounds composed of a four-interconnected pyrrole macrocycles. Normally, these macrocycles can be divided into three groups: porphyrins, chlorins, and bacteriochlorins. These organic compounds have different positions in which they can coordinate with different metal ions. These positions are the free nitrogens present in the central ring of the macrocycle, the β positions of the pyrrole, and the meso positions of the porphyrin (Figure 1.27).

These kind of metalloligands are widely used due to their intrinsic catalytic properties, as they are able to oxidize different organic molecules in mild conditions [93]. Also, the rings of the porphyrins are easy to modify by adding pyridines and carboxylic acids converting them into interesting building blocks for MOFs. Up to date, a large number of porphyrinic-MOFs have been synthesized with different modifications in the ligand such as the metal centers (Co, Cu, Ni, Zn, Fe, Mn) [94] or the different substituents along the axial positions of the metalloligand (F^-, OH^-, $O–CH_3$ among others) [92]. However, the principal problem of these complexes is that only a few of them show good stability for catalytic reactions [95], an issue that has been trying to be solved for a while [96–100].

Chemical Reactivity. The incorporation of porphyrins in MOFs can provide some advantages in catalysis, as they have intrinsic catalytic properties as mentioned before, and more particularly, if modifications are added to the ligand such as the incorporation of metals. Some examples of works published for catalysis with porphyrins include epoxidation reaction of olefins as exemplified in the work of Fujii et al. where they performed a Marcus plot analysis for the epoxidation reaction of the oxoiron (IV) porphyrin π-cation radical complex with alkene, to demonstrate the mechanism of the electron transfer, which occurs from the Highest Occupied Molecular Orbital (HOMO) of the alkene to the porphyrin π-radical orbital [101].

The hydroxylation of linear and cyclic alkanes is another typical reaction where a metalloporphyrin can be used as catalyst. As is the case in the work of Suslik et al. where they use a MOF called PIZA-3 with a metalloporphyrin as ligand to run the reaction of epoxidation of alkenes [102].

In another work, Hod et al. use a material that contains functionalized Fe-porphyrins as catalytically competent, redox-conductive linkers to perform electrocatalytic CO_2 reduction [103].

Bipyridyl ligands. Bipyridil ligands are metalloligands that contain bipyridine groups. Bipyridine is an organic compound consisting of two pyridyl rings. It is a bidentate chelating ligand that can coordinate with different transition metals giving rise to diverse complexes. There exist six different isomers, but two are the most used: 2,2′-bipyridine and 4,4′-bipyridine (Figure 1.28).

The bipyridyl ligands offer different and more versatile single-metal sites when anchored to them, than those anchored to porphyrin heterocycles [105]. Also, for this kind of metalloligands, single-metal sites can be directly synthesized or incorporated by PSM. The last case presents a problem as the metal salts of the precursors can form aggregates on the surface of the MOFs thus blocking the pores channels. Also, the formation of single-metal sites can be randomly distributed along the framework [106]. On the other hand, for the direct synthesis, these drawbacks are overcome as the metal species incorporated allow relative isolation and uniform distribution of the active sites along the MOF [107]. So, for these kind of ligands, the introduction of single-metal sites works better by direct synthesis approaches rather than by PSM, contrary to what is expected from what was said above [108].

Chemical Reactivity. The bipyridil ligands are also well used in catalytic processes, as they can host a large variety of metals as single-metal sites, as it is shown by Chen et al. where they use two different complexes of bipyridil ligand with Ru and Pt and they incorporated these two complexes into a robust MOF of Zr(VI) by mix-and-max approach. The incorporation of the complexes $[Ru(dcbpy)(bpy)_2]^{2+}$ and $Pt(dcbpy)Cl_2$ allows the facile arrangement of the photosensitizer and the reduction catalyst very close to each other which allows the promotion of the electron transfer between them, this improves the hydrogen evolution reactivity upon visible light irradiation [109].

Imine ligands. Imine ligands refer to ligands that contain a C=N bond in their structure. The unique electronic properties of this group make it a very interesting candidate for catalysis. The lone pair of electrons of the nitrogen atom can coordinate

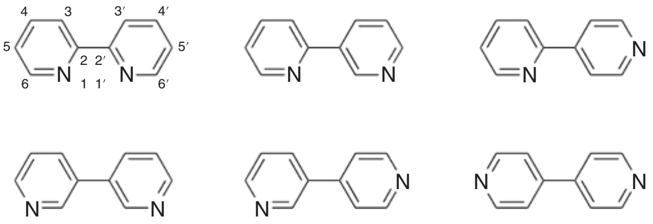

Figure 1.28 The different isomers of bipyridine. Source: Reproduced from Bipyridine [104]/Wikipedia/Public domain CC BY 3.0.

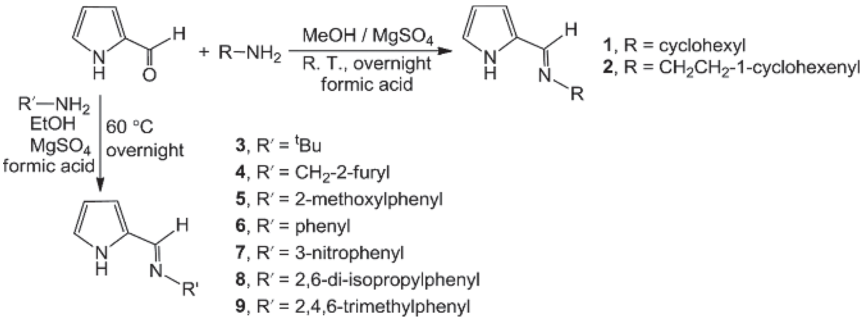

Figure 1.29 Synthesis of imine ligands. Source: Reproduced with permission from Chen et al. [110]/Elsevier.

to a large variety of metals. Imine ligands can be classified into three groups such as monodentate, bidentate, and polydentate imine ligands (Figure 1.29).

This type of metalloligands is commonly used because of its high stability in most organic solvents. It is obtained through a Schiff-based chemistry approach where a primary amine reacts with an aldehyde or a ketone under specific conditions, resulting in a replacement of the carbonyl group by an imine group. These Schiff reactions are an efficient and environmentally safe approach to generate homochirality. They are interesting because their nitrogen atoms can coordinate to different transition metal atoms, which makes them very convenient to perform as catalysts. Indeed, these kinds of complexes can be used as effective catalysts for organic reactions, mostly for asymmetric catalytic reactions. They also offer a large number of possibilities for post-synthetic transformations by metalation or conversion of the imine groups [111].

Chemical Reactivity. The use of the imine ligands in catalysis is quite frequent, since they provide a high stability. One example of the use of these kind of ligands in catalysis is the allylic alkylation reaction, as shown in the work of Ellman et al. where they use a *P,N*-sulfinyl imine ligand with Pd to form the complex. This material was utilized to carry out the catalytic reaction mentioned before with a high enantioselectivity (94%) [112].

Salen ligands. Chiral salen ligands are obtained from the condensation of diamines and aryl aldehydes. It was first described by Hugo Schiff in 1864 [113]. They are normally called Schiff base ligands and can coordinate metals through imino nitrogen and through different groups linked to the aldehyde. They are able to stabilize metals with different oxidation states which make them good candidates to perform as catalysts. This kind of ligand has four coordination sites and two axial ones. They are very similar to porphyrin ligands but can be prepared more easily, by simply condensation of amines and aldehydes in different solvents, and preferably with some dehydrating agent to favor the reaction (Figure 1.30).

Researchers normally use this kind of metalloligands with modifications on pyridyl or carboxylic groups, turning them into excellent building blocks for the formation of MOFs, and it has inspired the preparation of organic molecular switches-based MOFs. Playing with the chirality of these ligands, homochiral

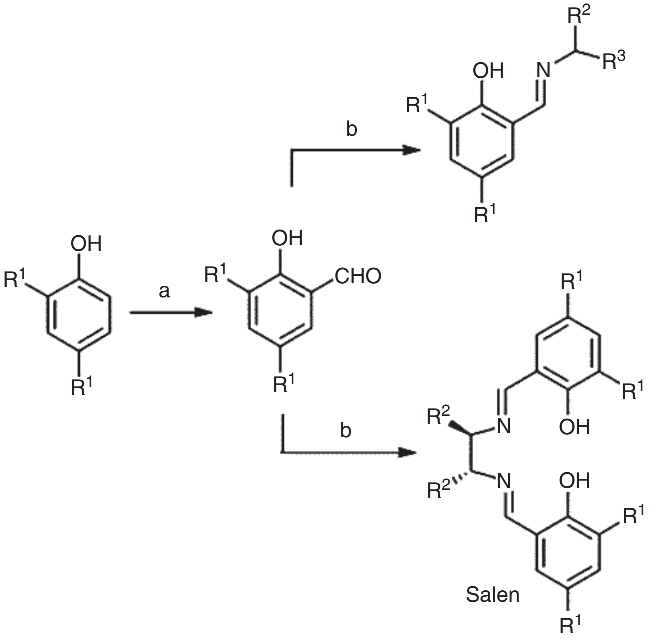

Figure 1.30 Preparation of Salen ligands. Source: Reprinted with permission from Cozzi [113]. Copyright 2004 Royal Society of Chemistry.

porous MOFs can be obtained by starting from enantiopure diamines, which give rise to chiral metallosalen ligands. These type of connectors have been considered one of the most important asymmetric catalysts to date [114–118].

Chemical Reactivity. A large number of people also use Salen ligands in catalysis, as they are very easy to modify with metals with different oxidation states. One example of a catalytic reaction performed through them is the Katsuki–Jacobsen epoxidation reaction. For that matter, Jacobsen et al. use a salen metalloligand to demonstrate the direct correlation of the asymmetric epoxidation reaction with the electronic properties of the ligand substituents [119].

Another interesting catalysis is the intramolecular acyl-transfer reaction. In this case, Nguyen et al. use a MOF with (salen) Mn complexes as ligand to carry out the reaction demonstrating that this metalloligand can enhance the catalyst stability and selectivity and allows its separation and reuse [120].

Metal-Free Organic Ligands. Although most mofs-based catalysts are catalytically active due to the metal or metals acting as active sites, there are also examples of metal-free ligand catalysis. The organic part of the MOF can be functionalized with different heterogeneous catalysts, as there are diverse functional groups that can act as active sites such as sulfoxy, pyridil, amino, and sulfonic groups, among others. Besides metal nodes, the functional groups of the ligands can also act as catalytic sites introducing acid and base catalytic activity [121]. The current catalytic processes use metals and metal oxides, however, there are different metal-free heterogeneous catalysts more efficient as they are less energy demanding and can compete with known conventional catalysts and even perform better than them.

Chemical Reactivity. As commented before, some organic ligands, and particularly, the majority of mentioned before, can act as catalysts by themselves, without the help of any metal. One example of this is the work published by Sanders et al. in which they use a cyclic porphyrin trimer as catalyst for catalytic acyl transfer. They create synthetic systems where the binding sites are positioned in a way where the substrate molecules are close in proximity, and they can catalyze reactions simply by their binding properties (Figure 1.31) [123].

1.2.1.2 Cooperation Between Single-Metal Sites and Metalloligands

The cavities on assemblies, like MOFs pores, –organic clusters, or some organic ligands, can stabilize reactive species for photocatalysis [124]. Also, they can enhance catalytic reactivities and selectivity by isolating guest molecules. So, bearing this in mind, the cooperativity among the different assemblies of the framework previously described and metalloligands can be used as homogeneous catalysts inside MOFs [125]. Combining their properties, they enhance the catalytic performance by having various heterogeneous catalysts in the same structure acting at the same time [126–128]. Immobilizing metal complexes into the organic ligands is one of the most convenient methodologies to prepare a MOF with different metal sites. Moreover, it can also offer high stability against the deactivation of the metal site.

Chemical Reactivity. Tandem reactions are frequently used in catalytic reactions due to their tuneable open metal centers (see Section 1.1), functional organic linkers, and active guest species in their pores (see Section 1.3). There are many examples as they are shown in the review of Cao et al. where they divide the tandem reactions into three categories: “(i) open metal centers and functional organic linkers, (ii) active guest sites in the pores and active sites in the MOF structure, and (iii) bimetallic nanoparticles (NPs) on MOF supports” [124].

1.2.1.3 Ligand Accelerated Catalysis (LAC)

Chiral ligands have gained a lot of attention due to the effects that they have on metal catalysis, which have been discovered and studied during the search of new metal-catalyzed asymmetric reactions. All of this has also led to the discovery of ligand-accelerated catalysis (LAC) [129] which consists of the addition of a specific ligand to an existing catalyzed process, improving the reaction time.

Chemical Reactivity. This phenomenon works for both homogeneous and heterogeneous catalysis. LAC is used in most of all catalytic reactions with transition metals. Some examples are guided by ligand exchange processes, which makes it possible that one single ligand could activate different catalysts inside a mixture of metals.

This phenomenon was discovered in 1988 by Sharpless and is found in the catalytic asymmetric reactions in Figure 1.32 [130]. But sometimes, there is a crowding around the catalytic sites, and this causes a deceleration rate, which is not desirable.

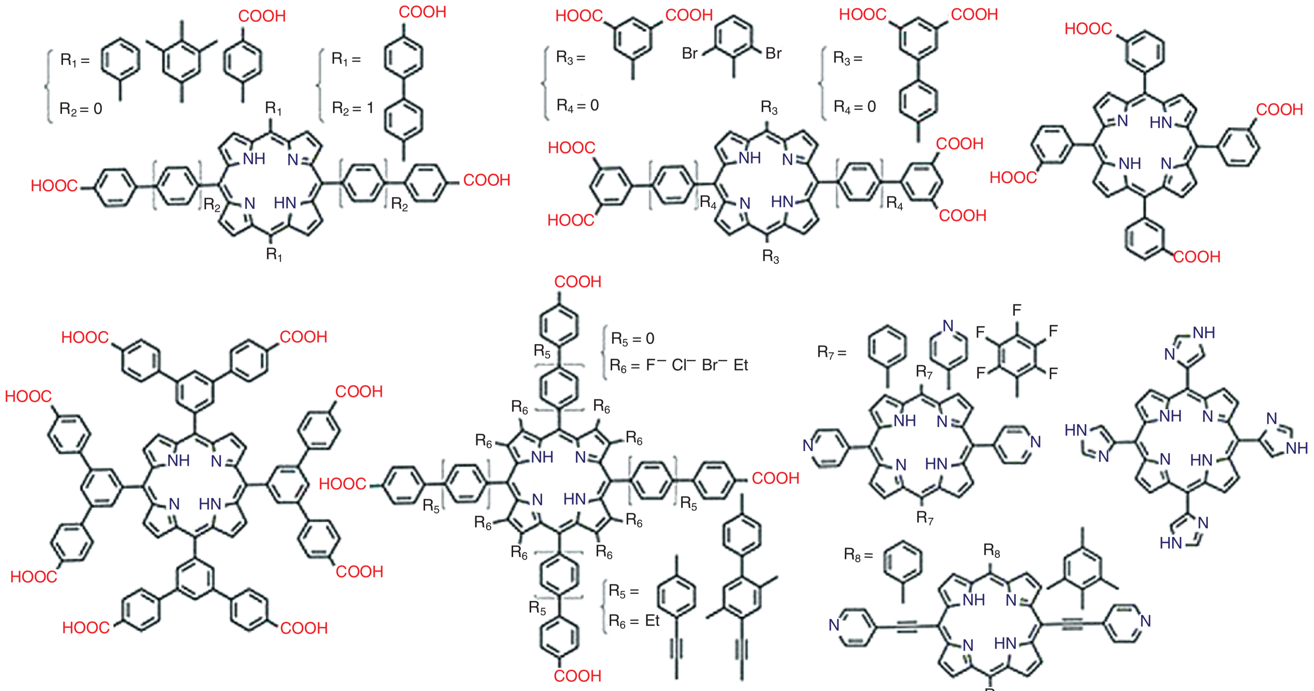

Figure 1.31 Summary of all metalloligands normally used in catalysis. Source: Reproduced with permission from Wei et al. [122]/American Chemical Society.

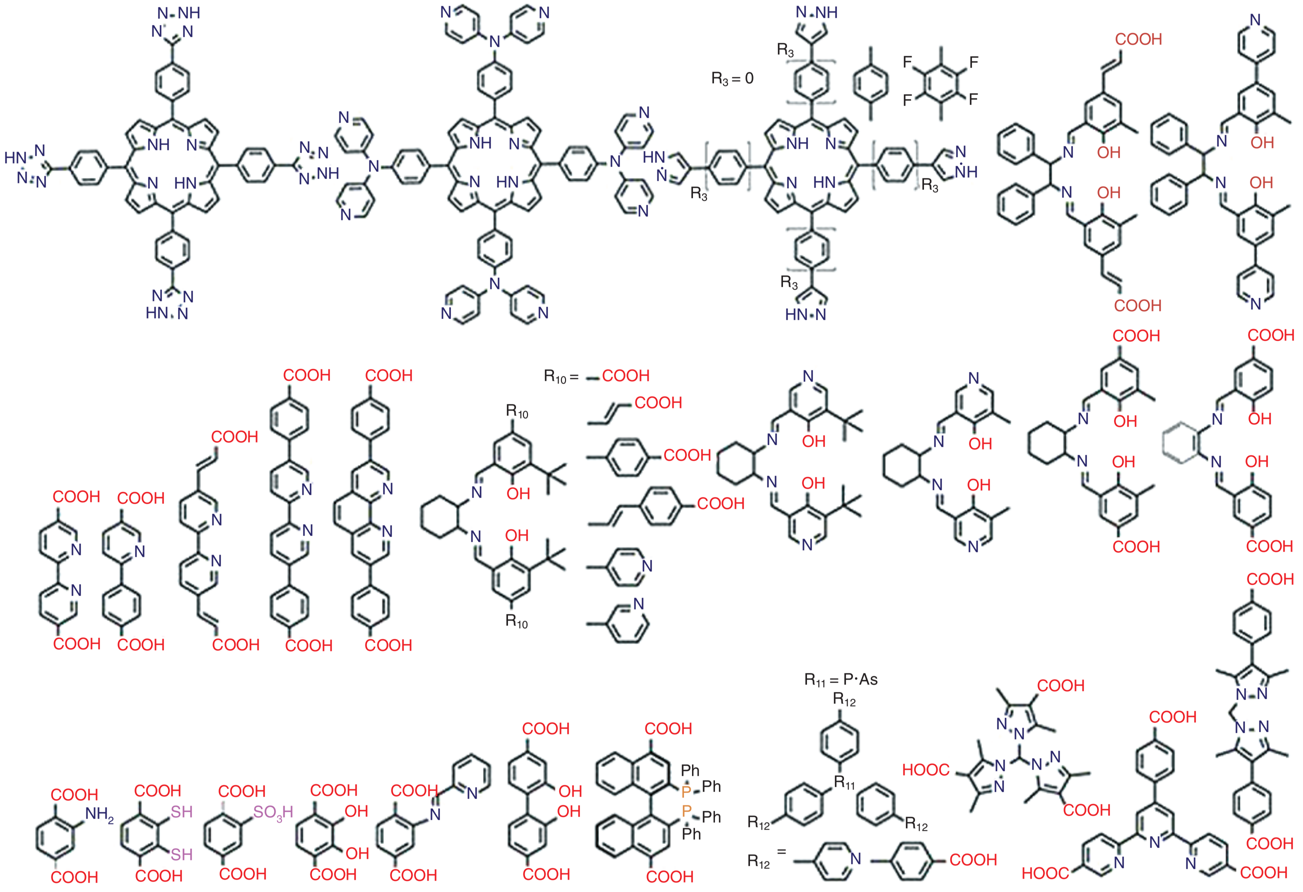

Figure 1.31 (*Continued*)

Entry	Olefin	Ligand, % ee,[b] confgn of diol[c] sign of $[\alpha]_D^{25}$	Time (h)
1	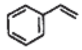	**1,** 62, *R*-(–) **1,** 60, *R*-(–) **2,** 53.6, *S*-(+)	3[d] 7[e] 7[e]
2	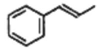	**1,** 65, *R*,*R*-(–) **2,** 55.4, *S*,*S*-(+)	5[d] 12[e]
3	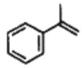	**1,** 33, *R*-(–)	1.5[d]
4	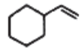	**1,** 46, *R*-(+)	1[d]
5	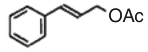	**1,** 76, *R*,*R*-(+)	7[d]
6	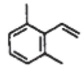	**1,** 65, (–)	3[d]
7		**1,** 20, *R*,*R*-(+)	17[d]
8	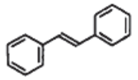	**1,** 88, *R*,*R*-(+) **1,** 85, *R*,*R*-(+) **2,** 78.5, *S*,*S*-(–)	7[d] 15[e] 17[e]

Figure 1.32 Some examples of ligands used in LAC. [a]All reactions were performed essentially as described for the molar scale process with stilbene. Specific notes and exceptions: (1) 1–5 mmol of olefin; (2) in small (ca. 7 ml) screw-cap vials (avoid rubber septa); (3) a temperature of 0 °C was maintained by storing the vials in an ice-bath for the duration of the reaction; (4) either 1 or 2 M in olefin as indicated (i.e. *d* or *e*). In all cases the isolated yield of the diol was 80–95%. [b]The enantiomeric excesses were determined by HPLC separation of the mono MTPA ester (entry 3), bis MTPA esters (entries 1, 2, 4–7), or the bis acetates (entry 8) in all cases by using a chiral Pirkle column (type 1A, preparative version) and eluting with *i*-PrOH/hexane. [c]The absolute configurations of the diols were established. For case 6, the correlation is not yet accomplished. Rotations were measured in EtOH except entry 5 which was taken in $CHCl_3$. [d][olefin] = 1 M and [Os] = 4×10^{-3} M. [e][olefin] = 2 M and [Os] = 4×10^{-3} M. Source: Reproduced with permission from Jacobsen et al. [130]/American Chemical Society.

1.2.2 Introduction of Metals by Direct Synthesis

The second part of this chapter is about the most common techniques used for the introduction of the metals into de organic ligands of the framework. *In situ* metalation, premetalation, and post-synthetic metalations are commonly used strategies to introduce metal active sites in the organic parts of MOFs.

This part of the chapter in particular will focus on the incorporation of the metal in the ligand by direct synthesis or by premetalation of the ligand and its subsequent incorporation into the framework that sometimes works better than the metalation by PSM, as it is more respectful with the conditions of the formation of the MOF.

The spatial arrangement of linkers can be elucidated by several techniques, but the choice of them will depend on the properties of the material. In these two last sections, we will also introduce some characterization techniques depending on the needs of each type of metalated ligand. It must be reminded that sometimes to obtain quantitative information about the ligands in the structure it is necessary to add an internal standard.

1.2.2.1 In-situ Metalation

In-situ metalation of the ligands in MOFs is a less used practice since it is not possible to know in advanced where the metal (that is desired to be in the ligand) will coordinate. There are a few reported works showing how to control the exact amount of metal added to the reaction to obtain a good incorporation into the ligand. Porphyrinic MOFs are the most used materials for this practice as they can have different coordination sites for the introduction of metals.

Chemical Reactivity. The in-situ metalation is not the most common technique used for catalytic processes but there are some examples where it is utilized as, for example, Zhang et al. reported a controllable synthesis of UNLPF-10, a porphyrinic MOF functionalized via *in-situ* metalation. They modified the metal/ligand ratio in order to control the extent of metalation within the MOF by varying this variable. The MOF obtained, exhibited channel-like pores along the crystallographic axes, as well as an enhanced performed in the photocatalytic experiments of oxygenation of sulfide. The results showed an increase in the rate of photo-oxygenation as the metalation ratio increased [131].

Characterization Techniques. In order to characterize the ligands that have been metalated *in situ*, in which you do not know what structure can be formed due to the addition of various metals at a time, Powder X-Ray Diffraction (PXRD) and Scanning Electron Microscopy, Transmission Electron Microscopy (SEM/TEM) are some of the characterization techniques than can help us solve this problem. This can be seen in the work previously mentioned by Zhang et al. where they use these techniques to characterize their material. With PXRD, they can determine the crystalline structure of the frameworks. This technique is also useful to visualize bond lengths, angles, and the coordination space at an atomic level. Furthermore, Single-Crystal X-Ray Diffraction (SCXRD) can be used to observe singles metal sites with host frameworks at different states such as defects [132]. Moreover, SEM/TEM and EDX are optical techniques that provide information about the morphology, chemical composition, and electrical behavior of a material. The chemical composition and the elemental distribution can be studied by EDX and mapping. Therefore, these techniques allow the extraction of the relative ratios for the linker and its distribution along the crystal [133, 134].

1.2.2.2 Premetalated Linker

On the other hand, premetalating the ligand and then introducing it in the MOF by direct synthesis is a more common practice. It involves a two-step reaction: first, a reaction to incorporate the metal into the ligand followed by another reaction to incorporate this into the framework. It is a longer work since it requires more steps but, most of the times, it is a more respectful procedure with the structure of the framework and the conditions for the formation of the same. There is a large number of reports that use this technique to introduce metals into the organic parts of the frameworks.

Chemical Reactivity. The premetalation of the ligands is a very used technique in the field of catalysis, as it allows to incorporate metals or metal complexes as metal sites for catalysis in a fast and safe way since it does not damage the original structure of the MOF. There are several examples of this kind of introduction of active metal sites like, for example, the work by Wu et al. who reported a Sn(IV) porphyrin MOF where they first metalled the porphyrin with Sn. They used this MOF for the photocatalytic reaction of oxygenation of phenols and sulfides, and they obtained quantitative yields for both reactions after four runs [135].

Another example of the same group was the one where they used the premetalated tetrakis(4-carboxyphenyl)porphyrin (TCPP) ligands with Mn and Ni and they combined these ligands with Mn(II) and Cd(II) ions to obtain the MOFs ZJU-18, ZJU-19 and ZJU-20. They used the MOFs for the oxidation of alkylbenzene and achieved the best results with ZJU-18 [136].

Characterization Techniques. Some of the characterization techniques that can help to know the nature of the ligand that has just been created by premetalation are the NMR and Mass spectroscopy. These are some techniques used in the work of Barron et al. where they use these to corroborate the ligand state [137]. In their work, they use in-situ NMR to monitor the composition of the liquid phase during the modification of the ligand of a Zr-MOF UiO-66.

Nuclear magnetic resonance techniques are divided into two blocks, those related to the liquid phase and those related to the solid phase (SS-NMR). The liquid phase is one of the most widely used technique to quantify the relative ratios in the structure of a complex, as well as to quantify the extent of the linker functionalization with another molecule [138]. On the other hand, SS-NMR is an effective tool to characterize the average distances and the distribution of linker. In this technique, it can be determined the chemical environment of a nuclei with a quantic number $1 \neq 0$ such as ^{1}H, ^{13}C, ^{15}N, ^{19}F, ^{31}P. It can provide a qualitative and quantitative analysis of the incorporated linker molecules and its functionalizations, and also, the linker distribution in the material.

Mass spectroscopy (MS) technique is used to obtain the mass-to-charge ratio of atoms or molecular fragments in the gas state. It is used to know the exact mass of any organic compound or complex mixtures by different methods such as ICP-MS, matrix-assisted laser desorption/ionization source with a time-of-flight mass analyzer (MALDI-TOF), accelerator mass spectrometry (AMS), thermal ionization-mass spectrometry (TIMS), or spark source mass spectrometry (SSMS). This technique is also commonly used in tandem with chromatography and other separation techniques to enhance the mass resolving/capabilities of the mass spectrometry. The only problem is that this is a destructive technique, so it is impossible to recover the samples [139].

1.2.2.3 Postgrafting Metal Complexes

In addition to the other two methods for the incorporation of metal complexes as active metal sites, another methodology to incorporate metal moieties is to synthesize a premetalated metal complex and then graft it into the organic ligands of the MOFs by covalent or coordination bonds [140, 141]. This approach has been used more recently than the others, but it holds great potential because it opens the door to the possibility to integrate well-defined metal complexes directly into the structure of the framework without any additional post-synthetical steps and helps to keep the structural integrity of the framework, avoiding degradation, and deactivation of the catalytic center as well [142].

Chemical Reactivity. The addition of metal complexes into the structure of a MOF by postgrafting is a common technique used to improve the catalytic behavior of the frameworks. There are several works published about this like the one by Ott et al. where they incorporate [Ru(bda)(L)$_2$] into a pyridine-decorated MIL-101(Cr) MOFs by the postgrafting method later exhibiting a tenfold increase in the turnover frequencies for water oxidation [143].

Characterization Techniques. For the characterization of ligands that have been modified by postgrafting metal complexes, one useful technique is X-Ray Photoelectron Spectroscopy (XPS). This is used to know if the metallic cluster created is introduced into the ligand retaining its properties, or if, on the contrary, it has been oxidized or reduced upon incorporated into the ligand. As reported by Shi et al., they use this technique to characterize the modification in the linker of the MIL-101-SO_3H-NHBOC and MIL-101-SO_3H-NH_2 and they saw their signals at a binding energy of 168.8eV which is consistent with the S^{6+} of the sulfonic acid group.

The fundamentals of XPS involve the detection of photoelectrons emitted from the sample as a consequence of the irradiation of the sample with X-ray photons. It can determine all elements through the detection of the binding energies of photoelectrons, with the exception of hydrogen and helium. As we have seen previously, this technique can give information about the chemical states of the species by small variations in the binding energies of the photoelectron lines as well as Auger lines satellite peaks. This way, XPS is a useful technique to obtain quantitative analysis of surface composition and to confirm the PSM of the linkers [144].

1.2.3 Introduction of Metals by Post-synthetic Modifications

Apart from the introduction of the metal by direct synthesis of the MOF or the premetalation of the ligand, there are other methods to introduce metals in ligands more commonly used by researchers, which are the PSM or post-synthetic metalations. In the last part of this section, we will detail the two post-synthetic methodologies most used for the introduction of metal active sites in the organic parts of the MOFs and the techniques of characterization usually used.

1.2.3.1 Post-synthetic Exchange or Solvent-Assisted Linker Exchange (SALE)

This efficient methodology is a ligand exchange strategy consisting of the replacement of certain ligands of the MOF by other metalloligands previously modified, which are in similar length, for the preparation of improved frameworks [145, 146]. These exchanges are normally carried out under milder conditions than direct synthesis. It is a proper route to control the spatial distribution of the building blocks, as during the process, the location of the linkers is determined by the synthesis conditions, so uniform and core–shell microstructures can be obtained, and the different spatial distributions of the building blocks lead to properties that cannot be achieved with the precursors of the pure MOF and can improve the application of these materials [147]. This methodology has been proven as a powerful tool to fabricate single-metal sites in MOFs for catalysis, due to the limitation of obtaining these kinds of materials by direct synthesis [121].

Chemical Reactivity. The SALE technique is a very used method to replace some ligands of a framework to other with different properties to enhance the catalytic properties of the MOFs, there are cases in which you can replace only some ligands of the structure and obtain a mixed-ligand MOF which combines the properties of both linkers, or you can replace all the ligands present in the structure. Some works as the one of Lillerud et al. explain how they do a linker exchange in an UiO-66 framework by changing benzoates by formate ligands, and it afforded a much more reactive material, which allows for the incorporation of different moieties important for the catalytic process [148] (Figure 1.33).

Characterization Techniques. Some useful characterization techniques to check if the ligand that has been replaced is in the right place and if it has not been damaged during the process are the Infrared (IR) and de UV–Vis. For example, Verpoort et al. [121] in their review show the use of IR and UV–Vis technique to characterize a MIL-101-Cr that has undergone a modification in its ligand. This modification involved a substitution of chlorine with imidazole,

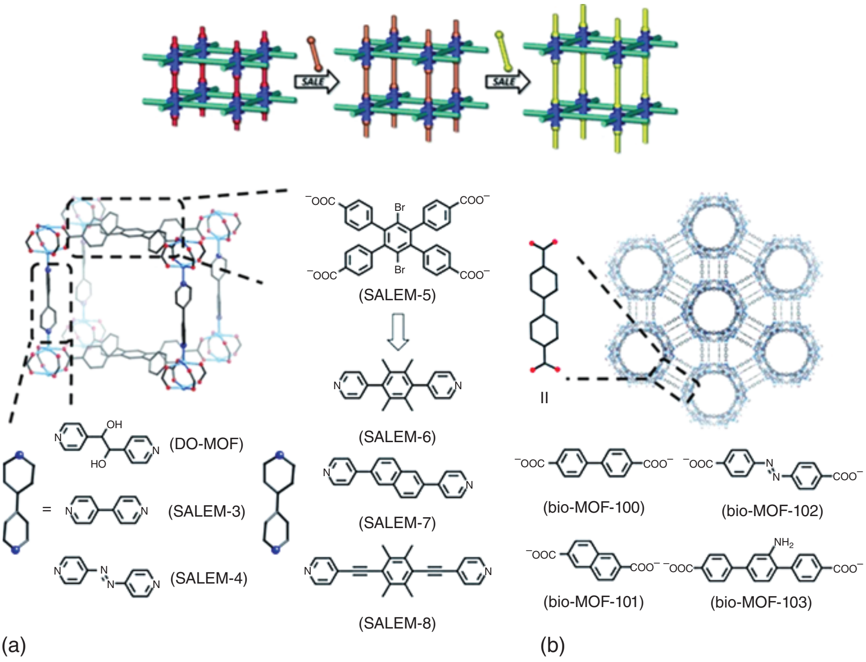

Figure 1.33 Top: Schematic representation of the incorporation of longer linkers into a MOF through SALE. Bottom: SALE in DO-MOF and SALEM-5 (a), and bio-MOF-101 (b). Source: Reproduced with permission from Karagiaridi et al. [149]/John Wiley & Sons.

used as a support for the immobilization of a catalysis moiety, a Mn(tcpp). They confirmed the presence of the complex by IR and UV–Vis. The resulting material, Mn(tpp)Cl@Im-MIL-101(Cr) MOF, is highly active, stable, and reusable for four consecutive runs without loss of catalytic activity.

Infrared spectroscopy is used to detect the adsorption bands of some molecules such as H_2, CO, NO, and CO_2. These molecules can be adsorbed on metal sites and present different vibrational frequencies and intensities when interacting with them, this is the way it can be demonstrated the presence of a single metal site in crystalline and amorphous materials [150]. UV–Vis technique is an absorption or reflectance spectroscopy that measures, as its name says, in the ultraviolet and the visible regions of the electromagnetic spectrum. It can be used to detect compounds that absorb in the range of the UV–Vis spectra, as for example chromophore ligands such as porphyrins. This technique is complementary to the fluorescence spectroscopy [151].

1.2.3.2 Post-synthetic Metalation

The precise incorporation of catalytic metal sites into MOFs by direct synthesis is a challenging thing, due to the difficulties in the synthesis of the MOFs, or the possible deactivation of the metal site during the direct synthesis, as mentioned in the introduction. That is why most people prefer to incorporate catalytic metal sites by PSM [152, 153]. This strategy normally involves mild conditions and has attracted people's attention lately [154]. This approach, consists of a two-step procedure, in which first a single metal bearing MOF assembly is prepared with the corresponding bifunctional ligand and then the introduction of a second metal ion occurs through a post-synthetic metalation resulting in a multi -metal MOF. This approach is usually chosen when the preformed complex would not handle the conditions required for the formation of the final MOF [155]. Usually, one of the organic ligands requirements to use the post-synthetic metalation is to have free chelating sites available at the functional groups, this is an important thing since these chelating sites would coordinate the different metal ions to form the active metal complexes for the catalysis. These single-metal sites can act as efficient heterogeneous catalysts in diverse organic reactions [156]. The post-synthetic metalation method has been broadly used in MOFs composed of different type of ligands such as pyridine, porphyrin, amine, thiocatechol, allyl, and phosphine groups as well as their derivative units and other organometallic species. An important thing to keep in mind is that monodentate functional groups are less stable for the chelation of metals than multidentate groups, the nature of metal binding in the first case is found to be difficult to elucidate and normally suffer from leaching of the metal species, but for the second case, these multidentate groups offer more stable chelating sites of the metal species. To date, a large number of metal precursors have been incorporated into the ligands of different MOFs using the post-synthetic metalation, to create diverse catalytic active metal sites [157, 158].

Chemical Reactivity. The post-synthetic modification is the most used method to incorporate metal moieties or other functionalization. There are a large number of works published using this methodology to add metal moieties for enhancing the catalytic properties of the MOF. One of them is, for example, the work of Cohen et al. where they use the PSM to introduce chelating sites in UMCM-1-NH_2 and then to metalate these sites with divalent (Cu^{2+}) and trivalent metals (Fe^{3+}), and the resultant MOFs UMCM-1-AMCupz and UMCM-1-AMFesal were used as robust catalysts for carbon–carbon bond forming reactions [159].

Characterization Techniques. To corroborate that the linker that has been modified post-synthetically has not suffered any damage during the transformation, there are some characterization techniques that can be helpful in seeing the composition and the chemical environment of the same, and they are the following: confocal microscopy coupled to Raman spectroscopy technique. This technique is used to determine the chemical composition along the crystal by measuring at different points and providing not only the chemical information, but also the microstructure. This way, the distribution of the linker along the crystal can be studied [160, 161]. Fluorescence lifetime imaging microscope (FLIM) technique can be complementary to the previous mentioned technique and supplies qualitative information about the spatial arrangement of the linker in the framework [162, 163]. Photo thermal induced resonance (PTIR) technique is the combination of two other techniques, IR-spectroscopy with lateral resolution of atomic force microscopy (AFM). This is another technique, complementary to the above mentioned, that can also provide information about the spatial ligand distribution. The technique provides this information by illuminating the sample at a fixed wavelength while the AFM tip scans the sample [164]. In an example of this, Kibria et al. published a work in which they use the Raman technique to corroborate the differences between two Zn-based MOF with different ligands, one with 1,2,4-triazole and other with 2-methylimidazole. In their work, they can see the bands of the in-plane bending modes and the bands of the C–H stretching of the azolate groups [160]. In another example published by Wuttke et al. they use the fluorescence imaging and lifetime analysis to determine the spatial arrangement of functionalities and the level of defects in a multivariable MOF UiO-67 [163]. Ramer et al. shows how the use of PTIR allows them to identify and obtain nanoscale images of the main components of each polymer they were working with, and also, their morphology when they have a mixture of them [164] (Figure 1.34).

Furthermore, there are some X-ray synchrotron radiation experiments that can shed some light in determining the coordination environment of the metal or metals

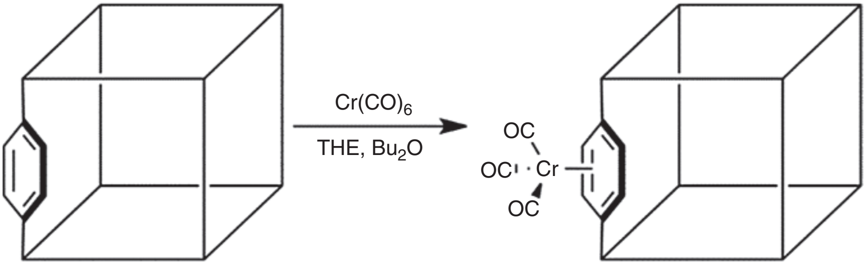

Figure 1.34 PSM addition by formation of organometallic chromium complex as demonstrated in MOF-5. Source: Reproduced with permission from Evans et al. [150]/Royal Society of Chemistry.

introduced in the framework and should be taken into account. These synchrotron techniques are useful for any type of metal introduced into the framework, either in the metal cluster (Section 1.1), in the organic ligand (Section 1.2), or in the cavities of the MOF itself (Section 1.3). The synchrotron technique referred to is the XAS, which can be further divided into EXAFS and XANES. On the one hand, Extended X-Ray Absorption Fine Structure (EXAFS) gives information about the distance and the number of the neighboring atoms as well as the chemical identity in the first coordination shell. This information can help in understanding the environment and chemical state of the metal in the organic ligand and material in general [165]. On the other hand, XANES provides information about the oxidation and the binding state of the metal, and also, the metal coordination geometry [166].

As it has been shown along the section, there are several ligands, metals, and techniques that can be used to introduce metal active sites in the organic ligands of the frameworks. As commented, there are a large number of characterization techniques to corroborate this. However, a comprehensive utilization of different techniques at a time for the structural understanding of the metal sites and their properties as catalysts is usually used. Moreover, more *in-situ* technologies to monitor the intermediates of the single-metal sites during the catalysis could be utilized, ultimately leading to a better understanding of the catalytic mechanism thus promoting the development of efficient single-site catalysts.

1.3 Metal-Based Guest Pore Engineering

According to the International Union of Pure and Applied Chemistry (IUPAC), porous materials can be classified as *microporous, mesoporous,* and *macroporous* depending on the pore size present within the materials. Microporous materials present a pore size smaller than 2 nm length, whereas mesoporous materials present a void width between 2 and 50 nm size [167–170]. Macroporous materials contain pore sizes bigger than 50 nm, so it is not relevant for the purpose of this chapter. MOFs usually present microporous or mesoporous porosity within their structure, which is important to bear in mind when encapsulating different molecules inside of them. The main challenge when immobilizing molecules in the pores is that some may not fit through; others may anchor themselves on the surface of the material or even aggregate before entering the cavities of the materials. For instance, just the porphyrin ring specie is estimated to be 0.84 nm in size not taking into account the delocalized electrons and the rigidity of the molecule [171], so the overall macromolecule would not fit through a micropore of the framework. In order to overcome these drawbacks, there have been many studies on the several approaches on how to immobilize different molecules within MOFs, not only after the material is already synthesized and the pore size is key, but also by growing the MOF around a guest that would not normally fit through the diffusion of the pores.

In this last part of the chapter, we will focus on the catalysis based on the different guests that can be encapsulated inside the MOF pores. As it has been previously mentioned, MOFs are organized crystalline structures with empty tuneable voids inside them that are able to immobilize and protect different catalytic species inside.

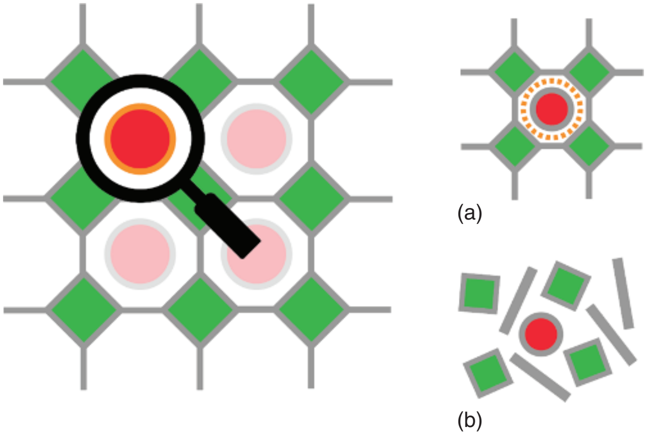

Figure 1.35 Schematic view of the two main general approaches to encapsulate molecular guests in MOF pores. (a) *MOFs as made*, by this approach we firstly synthesize the MOF and then we immobilize the guest; while (b) *In-situ encapsulation,* MOFs are grown over the guests by different strategies. Source: Figure produced by the authors of the chapter.

In this section, we will point out the distinct methodologies used either by *in-situ* encapsulation or by tailoring the pore size to store larger catalytic macromolecules. Furthermore, the various immobilization strategies of species, like metal NPs [172], polyoxometalates (POMS) [173], or large macromolecules (e.g. porphyrins) [171] will play a role in areas such as heterogeneous catalysis, photocatalysis, or electrocatalysis, among others. Overall, the summary of this chapter is represented in Figure 1.35.

1.3.1 Encapsulation Methodologies in As-Made Metal–Organic Frameworks

The large pore size distribution within MOFs makes them promising materials to capture guests with variable dimensions inside of them. In this approach, MOFs are made before the encapsulation takes place by conventional methodologies such as solvothermal synthesis where organic ligands and inorganic metal centers are mixed together in solution at room temperature or at high temperatures, depending on the desired MOF. Once we have obtained and washed the pristine materials, different methods are used to diffuse large molecules through the pores and immobilize them there. These methodologies could be considered as post-synthetical modifications, as the MOF is already formed when functionalized.

1.3.1.1 Incipient Wetness Impregnation

In this strategy, the already synthesized and activated MOF is submerged in a solution or gas flown containing an excess of the desired specie to be trapped by diffusion through the pores. The guest or precursor size is key as it has to fit across the cavities of the materials and stay there immobilized, thus it should not be too small or too big. One of the most common practical examples of this method is the encapsulation of large molecules such as POMS by the so-called incipient wetness impregnation. In this approach, the desired activated MOF with empty voids is submerged in an excess aqueous solution containing the POM specie [174]. Polyoxometalates are very interesting species due to their consideration as tuneable metal clusters which inside MOFs pores can be easily tailored by size, charge, or metal centers that will tune their properties making them more selective catalysts [175].

For instance, one of the first works of encapsulation of large molecules in porous materials is from Férey et al. in 2005 where they hydrothermally synthesized a Cr-based MIL-101 material with large pores sizes. After washing, activation, and characterization of the material, Keggin polyanions could fit through the voids and were incorporated by diffusion of the ion salts through the cavities [176]. The dried MOF was submerged in an aqueous solution of the Keggin salt for two hours. Moreover, the new composite material was successfully characterized to confirm the presence of the Keggin POM inside the MIL-101 (Cr). This study led to other impregnation of POMs reports for oxidative catalytic purposes such as the work from Kholdeeva et al. where they added an excess of M-POM (M=Co, Ti) to a Cr-based MIL-101 and successfully anchored the M-POM inside of the MIL-101 material [177].

On the other hand, not only POMs can be encapsulated within MOFs by incipient wetness impregnation. In a paper by Kaskel et al. in 2007, they described the immobilization of a palladium precursor inside the previously synthesized MOF-5 by this methodology (see Figure 1.37) [178]. The main difference among previous works is that in this case the guest precursor is subjected to the incipient wetness impregnation. First, they synthesized the material by solvothermal synthesis in autoclave at high temperatures, and then, once they had the MOF washed and activated, they slowly added the acetylacetonate palladium precursor dropwise with continuous stirring forming an orange paste. Subsequently, an evaporated solvent current was flown and evaporated for two hours in argon atmosphere, finally, letting the predried sample evaporate overnight to obtain the precursor MOF-5 material. After impregnation, the material was characterized to make sure

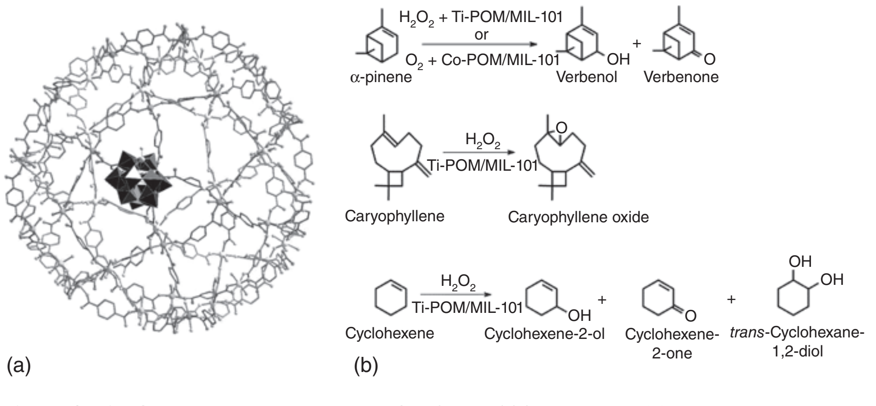

Figure 1.36 Schematic view of the M-POM@MIL-101 composite (a); and the cope of the oxidative catalytic reactions carried out in this study (b). Source: Reproduced with permission from Maksimchuk et al. [177]/Elsevier.

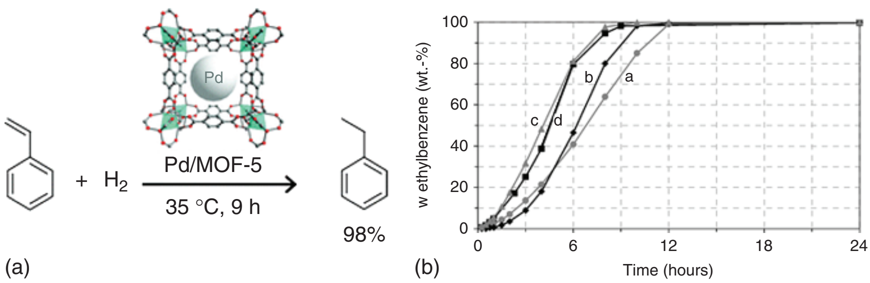

Figure 1.37 Hydrogenation reaction catalyzed by Pd@MOF-5 (a); and ethylene formation with time in the different Pd/MOF-5 studied in Kaskel's paper (b). The difference among the samples (a–d) is the drying method used for its obtaining. Source: Reproduced with permission from Sabo et al. [178]/Royal Society of Chemistry.

the precursor was diffused innards the micropores in order to thermally reduce the species precursor into Pd nanoparticles that fitted the cavities size.

A more complete study that followed Kaskel's work is a paper from Fischer et al. in 2009, where, by wetness impregnation and gas-phase infiltration, they diffused palladium precursors into Zinc-based MOF-5 followed by the thermally and photocatalytically reduction of the species into Pd nanoparticles, respectively.

Characterization Techniques. In all the examples, Cr-based MIL-101 and MOF-5 were characterized by common techniques for MOFs such as PXRD, TGA, and N_2 isotherms. On MIL-101-Cr, large pore sizes of 29 to 34 Å and Brunauer Emmer Teller (BET) surface areas up to 5900 $m^2\,g^{-1}$ were reported through the N_2 isotherms. The presence of the Keggin salt inside the MIL-101-Cr was determined by observing the differences between the initial and the final TGA weight loss, PXRD peak intensities, ^{31}P solid-state NMR, and N_2 sorption measurements. Herein, the decrease in BET surface area suggests a successful immobilization of the guests within the pores. IR was also used to confirm the integrity of the POM inside the MOF in both examples [176, 177]. By all these techniques, they could calculate the approximated number of 0.05 Keggin anions per chromium in the cluster in Férey's work [176].

On the nanoparticle examples, the Pd NPs inside MOF-5 were defined by the gradual decrease in the N_2 isotherms, the BET surface area, and the decrease in peak intensity in the PXRD patterns. Moreover, on the last work from Fischer, they do not only use the changes on the BET and PXRD to know if the nanoparticles are inside, but they also used Transmission Electron Microscopy (TEM) images to check the size and homogeneous distribution of the 2.4 nm Pd NPs within the MOF [179].

Chemical Reactivity. The composite formed by MIL-101 (Cr) and POMs was studied for selective alkene catalytic oxidations as can be seen in Figure 1.36b [177]. The stable material carried out the catalytic reaction successfully with high yields and good recyclability. In the other case mentioned, the Pd@MOF-5 was first utilized for hydrogen storage and then their catalytical properties were studied for the selective β-hydrogenation reaction of aromatic compounds as depicted in Figure 1.37. The reagents used were styrene, 1-octene, and *cys*-cyclooctene, but the optimization of the catalysis took place only with styrene. In Figure 1.37b, the four different composites formed by de Pd/MOF-5 are represented, where samples c and d show faster kinetic curves. Recyclability studies were also carried out showing a great stability of the material [178]. Lastly, on the work presented by Fischer, they performed the hydrogenation of cyclooctene but they do not focus on the catalytic properties of the composite rather on the characterization and optimization of the wetness impregnation technique itself by varying the loadings of palladium precursors into the Zn-MOF-5 [179].

1.3.1.2 Ship-in-a-Bottle

A more well-known strategy but similar to the incipient wetness impregnation would be the so-called *ship-in-a-bottle*. Herein, instead of impregnating the active specie directly into the material they diffuse the co-catalysts precursors through the pores. Once in the cavities, they would be transformed to form the immobilized catalytic species *in situ* inside the pores of the framework [180]. The name of the strategy comes from the guest being built inside the already-formed matrix material. The main challenge of this method would be the dispersion of the precursors inside the pores and not those getting stuck on the surface of the material, as in previous examples.

One early example of this would be the distribution of metal salts inside the pores in order to form metal nanoparticles by reduction inside the material. For instance, in 2012, Xu et al. used a previously reported double-solvent methodology to diffuse platinum-based salts inside MIL-101 (Cr) [181]. In this work, the previously synthesized Cr-based activated MOF, already mentioned, was dissolved in a dry non-polar solvent. The platinum salt was dissolved in an aqueous polar solvent and added dropwise into the stirring solution containing the MOF thus successfully achieving the inclusion of the platinum precursors in the voids. Afterward, the solution was left to reduce by increasing the temperature to finally obtain the Pt@MIL-101 composite with 2 nm Pt NPs inside of them.

Characterization Techniques. The MIL-101 (Cr) was characterized by PXRD, SEM, and N_2 adsorption. The key characterization technique carried out to certify the homogeneous distribution of the Pt NPs inside the MOF is TEM. As shown in Figure 1.38a,b, the Pt NPs size was also determined by TEM and fitted to a Gaussian distribution.

Chemical Reactivity. In order to prove the catalytic properties of this material, the catalytic performance was carried out for hydrogen generation reactions from the hydrolysis and later pyrolysis of ammonia borane. The studies show a high recyclability and efficiency not only in hydrogen generation reactions but also in gas-phase CO oxidation reactions. The main results from this work are summarized in Figure 1.38.

1.3.1.3 Metal–Organic Chemical Vapor Deposition (MOCVD)

Vapor deposition is a very well-studied synthetic methodology. In particular, metal–organic chemical vapor deposition (MOCVD), as its name recalls, consists of exposing a substrate to volatile precursors, being usually one of them

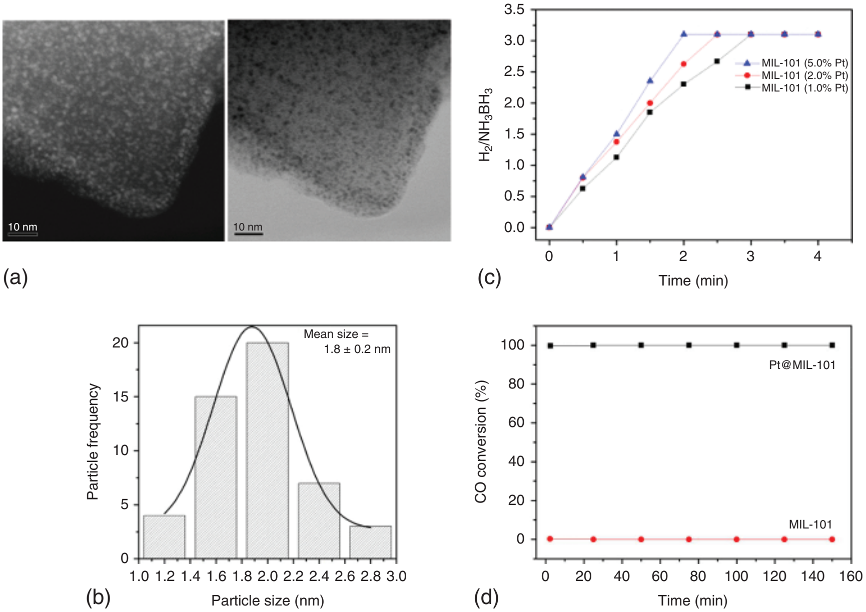

Figure 1.38 Summarize work of Xu et al. where (a) shows the TEM images of the Pt@MIL-101 composite, (b) histogram study on the Pt NP size distribution, and (c) and (d) are the catalytic studies on H_2 generation and CO oxidation, respectively.
Source: Reproduced with permission from Xu et al. [181], © 2012/American Chemical Society.

an organometallic compound, in order to be deposited onto the surface. These precursors usually react or decompose thus placed on the support. It can also be called MOCVD [182]. For the purpose of this chapter, our common substrate would be the porous frameworks while the organometallic volatile compounds are the desired guest to be embedded in the pores. Haruta et al. presented one of the earliest works on this methodology in 1997 for the preparation of gold catalysts anchored onto the surface of TiO_2 [183]. It was not until the following year where an example of CVD was reported for the deposition of gold nanoparticles in molecular sieves for catalytical applications [184].

However, examples of encapsulation of guest molecules inside MOFs by CVD came later in 2005 in a work by Fischer et al. where they propose to use MOF-5 as an absorption matrix suitable for the immobilization of metal–organic precursors by vapor deposition [185]. In this work they synthesized the previously mentioned along this chapter, Zn-based MOF-5 by solvothermal methodologies following the initially reported synthesis by Yaghi et al. Once the MOF-5 was dried and activated, it was exposed to the vapor of the organic palladium, copper, and gold precursors separately under vacuum and room temperature in a Schlenk tube. A color change was rapidly observed in the powder from colorless to dark red within five minutes in the case of Pd, and similar with the other two metal analogs. The metal–organic precursors are held inside the pores by weak interactions with the Zn cluster without

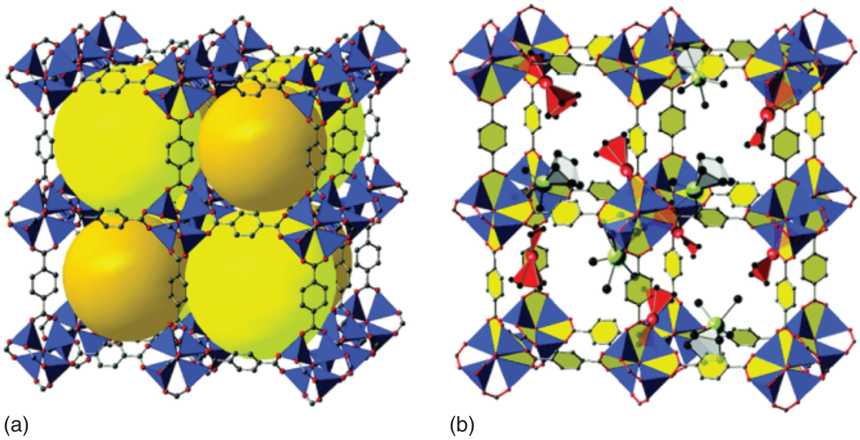

Figure 1.39 MOF-5 unit cell (a); and $[L_nM]_a$@MOF-5 showing how the guest interacts inside the voids (b). Source: Reproduced with permission from Hermes et al. [182]/Royal Society of Chemistry.

altering the crystallinity or surface area of the whole material. Afterward, a hydrogen gas flow was introduced and therefore reducing the metal species to nanoparticles guests inside the cavities obtaining MNPs@MOF-5 materials (M=Pd, Cu, Au). A similar work was published in 2006 by the same authors but doing a greater scope of organic precursors in the CVD inclusion [182]. Fe, Pt, Pd, Au, Cu, Zn, and Sn precursors were utilized to acquire $[L_nM]_a$@MOF-5 compounds where they attributed their immobilization to weak Van der Waals forces between the Zn and them, seen schematically in Figure 1.39.

A more recent work by Kempe et al. uses the CVD strategy to embed Ni/Pd NPs inside MIL-101(Cr) [186]. Furthermore, they successfully achieved different loadings of Ni/Pd precursors inside the MOF cavities. Following a previously described CVD methodology, the MIL-101 powder was activated and a flowed of organic Ni/Pd organic precursors passed across in the gas phase under vacuum by simultaneous or successive loading of the precursors. Afterward, a hydrogen gas flow was introduced to obtain the metal NPs inside the voids. They observed that, depending on the loading approach, the metal contents and the NPs formation were different thus affecting the overall properties of the Pd/Ni@MIL-101 composite. Successive loading led to bigger NPs that were anchored on the surface rather than inside the material. On the other hand, simultaneous loading of the precursors guided the formation of Pd/Ni bimetallic NPs, which size was adapted to the MOF cavities. The materials obtained by this were Pd_4Ni_1@MIL-101 and Pd_3Ni_2@MIL-101.

Characterization Techniques. The M@MOF-5 composites formed in the work by Fischer et al. were characterized by conventional techniques such as PXRD, SEM, and their surface areas were calculated by Langmuir models in N_2 isotherms. The metal NPs size was determined by the width of the PXRDs where the main profile remains intact. TEM images estimated the Pd NPs size to be 1.4 nm, while the Cu ones were of approximately 3–4 nm. The Au NPs are the most polydisperse as their size goes from 5 to 20 nm. The calculation of guests per pore was made by elemental analysis measurements, which resulted to be between 2 and 4 species per cavity. The $[L_nM]_a$@MOF-5 from the next example from Fischer showed a more detailed characterization of the materials obtained using atomic absorption spectroscopy (AAS) to determine quantitatively the metal content inside the material. In addition, FT-IR, solid-state NMR spectroscopy, or PXRD were utilized as complementary techniques to prove the presence of the Van der Waals forces with the Zn centers (see Figure 1.40 below). In the last example, from Kempe et al., elemental analysis was carried out to get an estimated metal loading of approximately 20% in all the materials. Pd_4Ni_1@MIL-101 and Pd_3Ni_2@MIL-101 showed a decrease in the N_2 adsorption isotherms whereas the Pd@MIL-101 and Ni@MIL-101 remained similar in large surface areas.

Chemical Reactivity. The catalytic experiments shown in Fischer's work focused on methanol production from gas synthesis and hydrogenation of cyclooctene. Results exhibit a moderately active performance for Pd@MOF-5 and Cu@MOF-5. However, Au@MOF-5 did not display any catalytical activity due to the aggregation of the Au NPs inside the MOF. Following Fischer's work in 2008, another article was published where they immobilized Ruthenium NPs inside MOF-5 by CVD [187]. Although similar to previous publications, in this work a more in-depth study on the catalytical properties of the final materials was studied. They carried out the oxidation of benzyl alcohol following its evolution by Gas Adsorption/Mass Spectroscopy (GC/MS) and the hydrogenation of benzene using the Ru@MOF-5 material as catalyst. However, the sensitivity of MOF-5 to water gave them unsuccessful results for the oxidation of benzyl alcohol.

In the study of Pd/Ni@MIL-101, these materials demonstrated to have great catalytical applications. Hydrogenation reactions were carried out with phenol and cyclic ketones/dialkyl ketones. The composites obtained by 1:1 successive loading showed lower catalytic activity and conversion. Nevertheless, Pd_4Ni_1@MIL-101 and Pd_3Ni_2@MIL-101 exhibited a synergetic catalytic effect that gave them a significant conversion capacity, enhanced stability, and higher reusability under aggressive conditions compared with the Pd or Ni@MIL-101 materials. The hydrogenation of

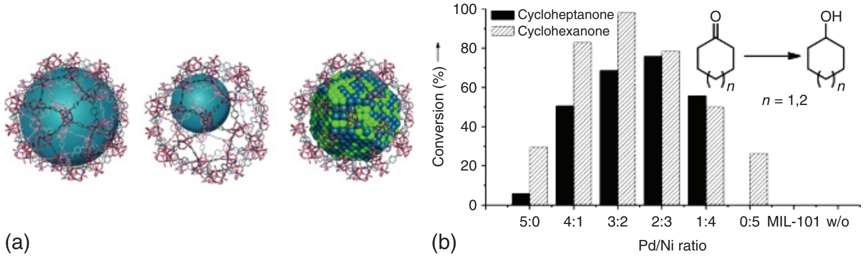

Figure 1.40 Simulation of the formation of the singles MNPs adapted to the MIL-101 cavities and the bimetallic NPS within the voids (a); and catalytic hydrogenation of phenol showing the % conversion with the different bimetallic NPs ratios (b). Source: Reproduced with permission from Hermannsdörfer et al. [186]/John Wiley & Sons.

dialkyl ketones was only feasible with the Pd_4Ni_1@MIL-101 and Pd_3Ni_2@MIL-101, which is attributed to their synergetic effect.

1.3.1.4 Metal-Ion Exchange

This encapsulation strategy is relatively new as the first example was published by Ma et al. in 2014 [188]. Their approach has similar characteristics that the one explained in Section 3.1.1: incipient wetness impregnation. However, the main variance is that the solvent from the impregnation is not evaporated. The previously synthesized MOF is submerged into the metal species they want to exchange without stirring and letting them decant at room temperature for some time. Afterward, small fragments of other components are anchored to the ionic centers.

In this specific example, Ma et al. synthesized bio-MOF-1 by reported methodologies consisting of mixing Zn salts with adenine and introducing an organic ligand such as biphenyldicarboxylic acid. The final material is a crystalline MOF where the SBUs are formed by zinc and adeninate species with organic ligands holding the cluster columns together [189]. This MOF-based material forms an anionic structure whose counterions are dimethylammonium cations originated from the decomposition of DMF and water molecules. Once bio-MOF-1 is acquired, the anionic material is submerged in a Co (II) acetate cation methanol solution for eight hours at room temperature. Therefore, a metal-ion exchange has taken place where the counterions have been replaced by positive charged metal centers such as Co, Ni, or Cu. The material is washed to avoid anchoring of metallic species onto the surface. Once the metallic centers are inside, they proceed to carry out a further functionalization by adding an organic linker in order to occupy the remaining place within the nanospace. The anchoring of the 1,2-dicyanobenzene (DCB), ligand is directed by the cationic metal center present. Moreover, they tried other encapsulation procedures to get the same materials, but they were unsuccessful (see Figure 1.41 below).

Characterization Techniques. In these works, conventional techniques are used to fully characterise the material such as PXRD, N_2 adsorption, XPS and MS. First, PXRD was used to check the integrity of the crystalline structure. ICP-MS, elemental analysis and MS confirmed the complete ion-metal exchange and the

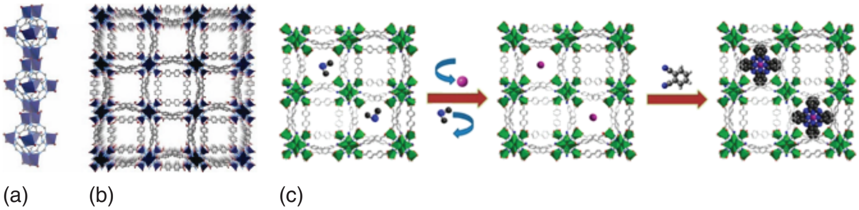

Figure 1.41 SBUs anion column formed by the Zn metal centers and the adeninates (a); crystalline structure of bio-MOF-1 (b), and schematic representation of the metal-ion exchange encapsulation process, with directional bonding of the organic linker at the end (c). Source: Adapted and reprinted with permission from An et al. [189]. Copyright 2009 American Chemical Society; Reproduced with permission from Li et al. [188]/American Chemical Society.

formation of the Co-Pc guest inside the nanospace. The BET surface area calculated through N_2 adsorption isotherms resulted in a decreased on the surface area due to the high occupancy of the pores. Complementary techniques such as XPS or UV–VIS were utilized to further verify the formation of the Co-Pc.

Chemical Reactivity. Catalytic styrene epoxidation was studied and the results were compared to ones obtained with the pristine material to see the enhancement of the process. Co-Pc@bio-MOF-1 material showed a 72% conversion and a 65% selectivity whereas bio-MOF-1 exhibited only an 8% conversion, under the same reaction conditions. No metallic leaching was observed in the brand-new composite material, which could be reused up to 3 times without decreasing its catalytic activity.

1.3.2 *In Situ* Guest Metal–Organic Framework Encapsulations

In this final section, called *in-situ* methodologies for encapsulation, the common characteristic would be that the precursors forming the MOFs and the chemical species desired to be immobilized are mixed and grown together at the same time to form the final composite *in situ*. In this approach, the guest size is not as significant as for the final material obtained. There have been different studies and classifications of the methodologies; however, we will summarize and give examples of the main approaches with the broad range of species used such as POMS, metal-NPs, enzymes, etc. [190, 191].

1.3.2.1 Solvothermal Encapsulation or One Pot

Amongst all the encapsulation techniques, solvothermal encapsulation or one-pot synthesis is the most commonly used out of them all. This strategy is very similar to the pristine synthesis of MOFs itself. The main characteristic is the mixing in solution of the metal precursors and the organic ligands of the desired MOF with the guest molecules, which are aimed to be embedded inside the pores.

As we have previously mentioned, porphyrins are large molecules, especially challenging to diffuse through the pores of already synthesized MOFs. Due to this, a lot of studies have been focused on these species. One early example of this inclusion method is a work by Vetromile et al. in 2011 where they successfully synthesized M-HKUST (M=Cu or Zn) with a metalloporphyrin embedded in its mesopores [192]. In this publication, they report the first metal–organic material enzyme (MOMzyme-1) by mixing the Hong Kong University of Science and Technology (HKUST) precursors with the porphyrin of choice and letting them react at 60 °C during seven hours. The porphyrins trapped inside the pores were functionalized in a second step with metal centers such as iron or manganese, mimicking the active site of some enzymes. Furthermore, these cationic centers are capable of exchanging themselves with other cationic metal centers which makes them able to tune their catalytical properties. The MOMzymne-1 still shows considerably enhanced porosity while protecting the porphyrin inside while small molecules can still pass through the small cages in HKUST in order to reach the porphyrin metallic center. Inspired by this methodology, a more recent work by Sun et al. shows the promising catalytic potential of these materials to convert CO_2 into more interesting products such as C_2H_4, which will be explained later in the chemical reactivity subsection below [193]. In this case, following the reported synthetic methodology, composites formed by M-TCPP porphyrins and Cu-MOFs were obtained by mixing BTC ligand with the metal-based porphyrin (Fe, Co, and Ni based) in an ethanol-DMF solution and added to the aqueous copper precursor solution. This mixture was left to react in an autoclave at 60 °C for 12 hours. Finally, five products were successfully acquired, one with the non-metalated porphyrin and the Cu-MOF and, the other four compounds with iron, cobalt, nickel, and copper porphyrin centers, respectively, inside the MOF cavities.

Another significant work to bear in mind in this approach is a publication from Hupp and coworkers where they selectively encapsulated different nanoparticles inside ZIF-8 by the one-pot methodology [194]. The main difference with previous examples is that in this work they do the encapsulation at room temperature. Herein, they achieve the synthesis of a big scope of nanoparticles with different sizes, shapes and compositions. Afterward, these nanoparticles were stabilized with organic components, such as polyvinylpirrolidone (PVP). Their goal was to use the stabilising organic compound to anchor the MOF precursors and start growing the MOFs over the metal-nanoparticles. This methodology could also be denominated build a "bottle-around-ship". Moreover, they successfully optimized the controlled encapsulation of NPs by adding different concentrations of them to the ZIF-8 precursors in methanol and letting them react at room temperature without stirring for 24 hours. In this work, they obtained Pt@ZIF8, Au@ZIF-8, Ag@ZIF-8, among other composites without altering the intrinsic porosity or crystallinity of the material, as you can see in Figure 1.43.

Characterization Techniques. As these are *in-situ* methodologies typical MOF characterisation techniques are utilised (PXRD, SEM, TEM, EDX, TGA, and N_2 isotherms). In contrast with previous approaches where the MOF can be characterized before forming the host-guest material, in this case the comparison is between the final functionalized material to the pristine MOF made in different synthetic batches. In the M-TCPP@Cu MOF work they use several techniques such as TGA to study the stability of the newly formed composite and, SEM and PXRD to check that the morphology and crystallinity of the initial porous material is maintained. But more importantly, to characterize the guest molecules, they use EDX-Mapping to check the porphyrin metal distribution within the material and, complementary, IR spectrum for the presence of characteristic porphyrin peaks such as C-H pyrrol bending at 1004 cm^{-1}. XPS studies were performed to check the chemical composition and their elemental state in the electrocatalysis. Results showed a reduction in the Cu centre from Cu^+ to Cu^0 which intervenes in the catalytic reaction, but the integrity of the material is maintained during the whole process. Furthermore, in the work from Sun et al. they mainly focused on the use of optical techniques such as HRTEM, SEM or EDX, to confirm: first, the formation of the nanoparticles previously synthesized and, consequentially, the homogeneous distribution of them inside ZIF-8, as you can see in Figure 1.43b. It is important to highlight that the presence of the different NPs does not alter the N_2 adsorption isotherms and neither the BET surface area obtained for the NP@ZIF-8, which are comparable to the pristine ZIF-8 itself.

Chemical Reactivity. In the work from Sun et al. once the materials were fully characterized, they were transferred to electrodes in order to carry out the electrochemical catalytic experiments. The proposed mechanisms for these consist of small molecules of carbon dioxide reaching the metal-porphyrin center through the pores where they were reduced to carbon monoxide in order to finally arrive at the copper MOF cluster to be transformed to ethane, as you can see in Figure 1.42. The enrichment of the Cu-MOF with copper metal centers in the porphyrins enhances the catalytic performance of the material compared to other previous composites obtained. Additionally, in Sun's paper, they studied the heterogeneous catalytic performance of the brand-new composites by the oxidation reaction of carbon monoxide and the hydrogenation reaction of alkenes such as *cis*-cyclooctene or *n*-hexene, see Figure 1.43.

1.3.2.2 Co-precipitation Methodologies

There are not many examples of this synthetic strategy as it is very similar to the one pot methodology which can difficult its differentiation. In previous methodologies, the main idea was to mix the precursors and the already synthesized guest together in order to obtain the final material. However, in a study by Kaskel et al. from 2007, they made this subtle difference [195]. Kaskel reported the preparation of palladium nanoparticles supported on MOF-5 composite, inspired by a previous work from Huang and coworkers consisting on the preparation of a Zn based metal-organic coordination polymer (MOCP) by what they called "direct mixing" strategy in a short period of time [196]. In order to do this, Kaskel and coworkers prepared a mixture of zinc nitrate hexahydrate salt, 1,4-benzenediccarboxylic acid and palladium nitrate trihydrate precursors by dissolving them in organic solvents at 60 °C and vigorous stirring. A precipitated was formed, dried and washed several times to obtain the pure Pd@MOF-5 material, without further modifications.

Characterization Techniques. The materials acquired were characterized by PXRD, nitrogen adsorption isotherms at 77K, and SEM. The highlighted technique from this work is the quantitative determination of the palladium content by AAS. Because of the fact that there were no significant differences in the isotherms, the AAS technique is the only probe that confirms the Pd supported in the MOF.

Chemical Reactivity. Catalytic hydrogenation reactions were performed in liquid–gas phase to see the applicability of this material. Hydrogen is in the gas phase while the reagents and the composite catalysts are in the liquid phase. Hydrogenation of ethyl cinnamate with the Pd@MOF-5 synthesized by this methodology showed an enhancement in activity compared to the Pd/C commercial catalyst with the same loading of Pd. However, it was observed after one cycle a complete loss in micropore volume without decreasing the catalytic activity.

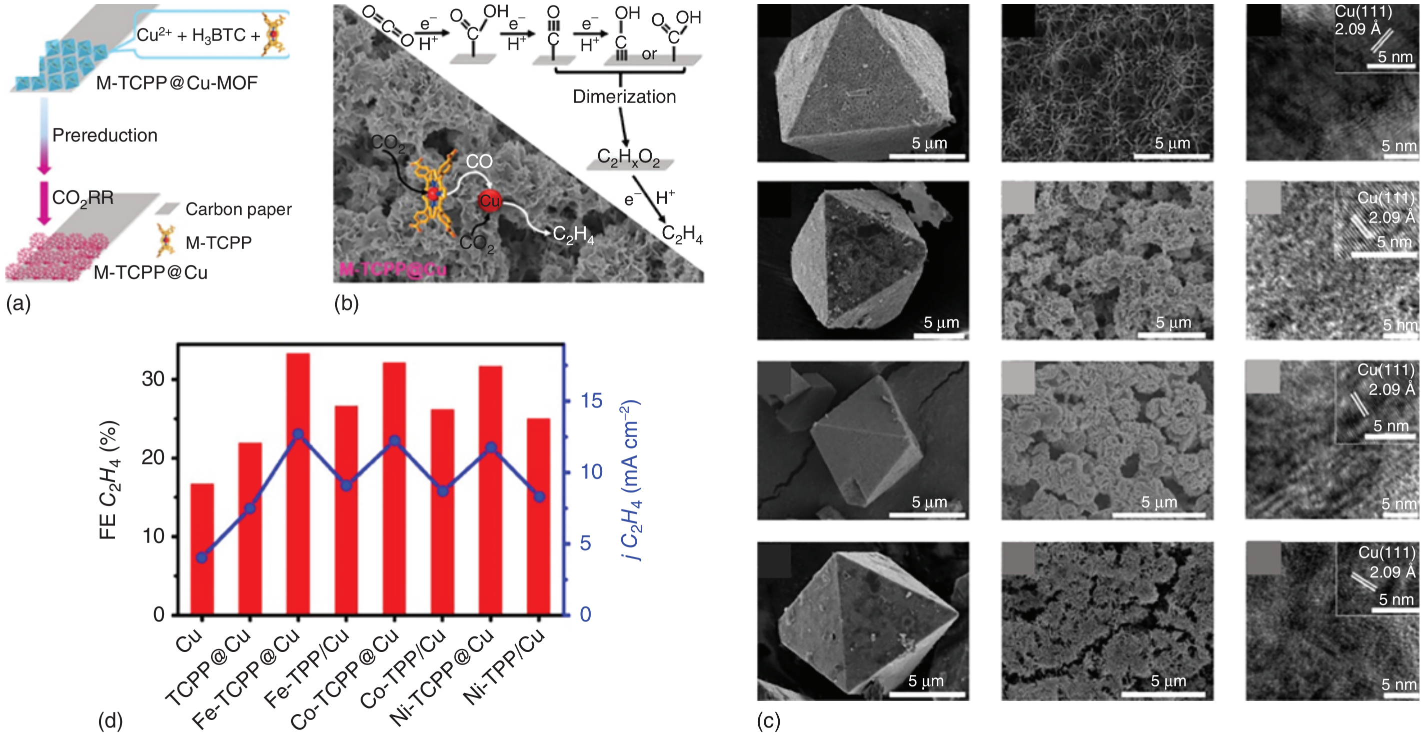

Figure 1.42 Schematic view of the synthetic mechanism proposed for the M-TCPP@Cu MOF (a); schematic view of the proposed catalytic mechanism with the enhancement provoked by the M-TCPP present (b); SEM and HRTEM images of the different composites obtained with the coral distribution inside the material (c); and C_2H_4 catalytic results from the different materials obtained (d). Source: Reproduced with permission from Sun et al. [193], © 2021/American Chemical Society.

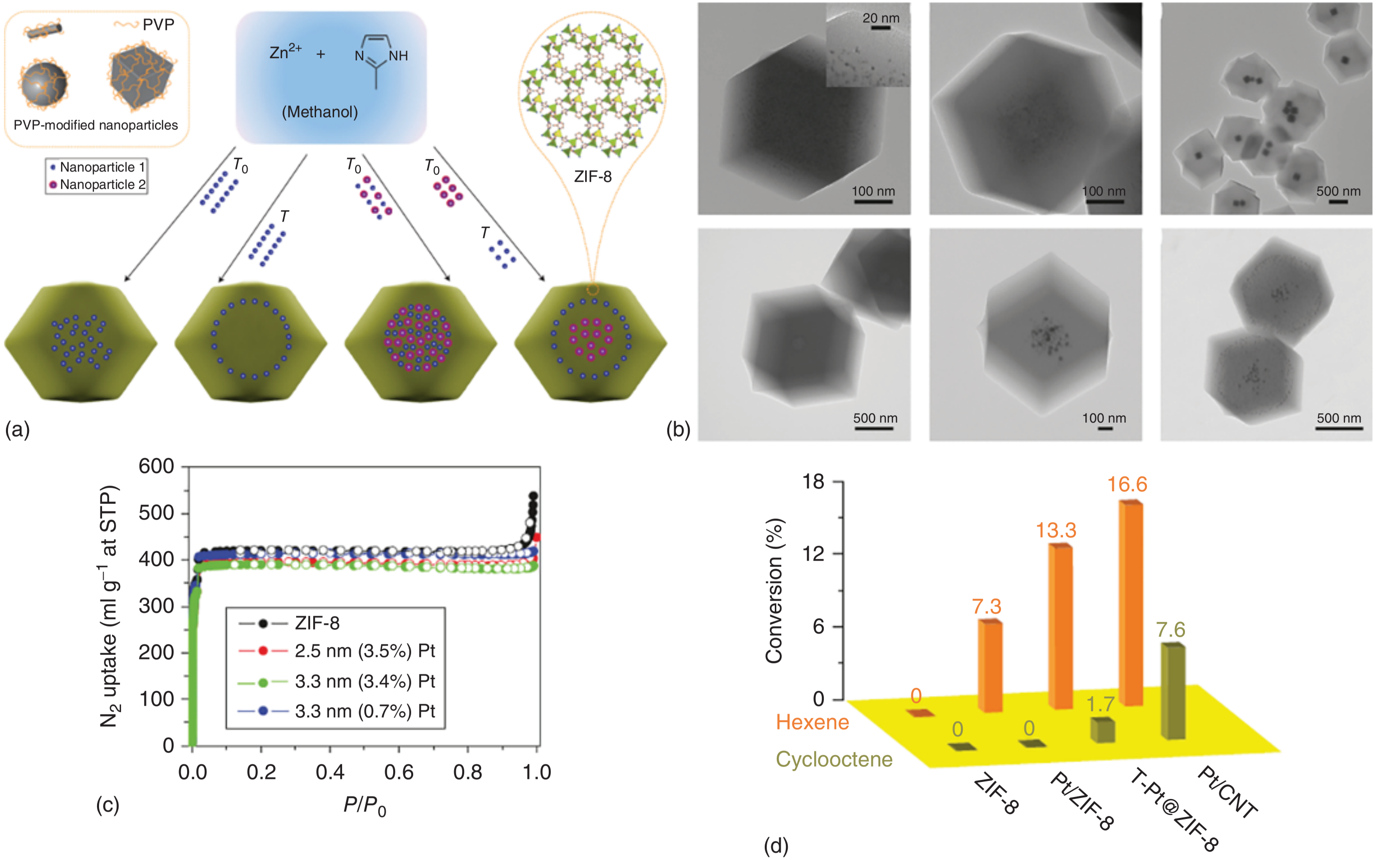

Figure 1.43 Schematic view of the controlled encapsulation of different nanoparticles in ZIF-8 by adding one type of NPs or two types of NPs (a); TEM images of the different NPs@ZIF-8 formed (b); N_2 isotherms of the Pt NPs@ZIF-8 composite where they observed no differences among them (c); catalytic performances of the Pt@ZIF-8 composites in the hydrogenation studies (d). Source: Reproduced with permission from Lu et al. [194], © 2012/Springer Nature.

List of Abbreviations

AAS	Atomic Absorption Spectroscopy
AFM	Atomic Force Microscopy
AIM	Atomic Layer Deposition in Metal–Organic Frameworks
ALD	Atomic Layer Deposition
AMS	Accelerator Mass Spectrometry
BET	Brunauer Emmer Teller
BTC	1,3,5-benzenetricarboxylic acid
DCB	1,2-dicyanobenzene
DFT	Density Functional Theory
EDX	Energy-Dispersive X-ray Spectroscopy
EXAFS	Extended X-Ray Absorption Fine Structure
FLIM	Fluorescence Lifetime Imaging Microscope
FTIR	Fourier-Transformed Infrared Spectroscopy
GC/MS	Gas Adsorption/ Mass Spectroscopy
HKUST	Hong Kong University of Science and Technology
HOMO	Highest Occupied Molecular Orbital
HRTEM	High Resolution Transmission Electron Microscopy
ICP-MS	Inductively Coupled Plasma-Mass Spectrometry
IR	Infrared Spectroscopy
LAC	Ligand Accelerated Catalysis
MALDI-TOF	Matrix-Assisted Laser Desorption/Ionization source with a Time-of-Flight
MCD	Missing Cluster Defects
MIL	Material of the Institute Lavoisier
MLD	Missing Linker Defects
MM-MOF	Mixed-Metal Metal–Organic Framework
MOCVD	Metal–Organic Chemical Vapor Deposition
MOCP	Metal–Organic Coordination Polymer
MOF	Metal–Organic Framework
MOM	Metal–Organic Material
NMR	Nuclear Magnetic Resonance
NPs	Nanoparticles
OMS	Open Metal Site
PDF	Pair Distribution Function
PIZA	Porphyrinic Illinois Zeolite Analogue
POMS	Polyoxometalates
PSM	Post-synthetic Modification
PTIR	Photo Thermal Induced Resonance
PVP	Polyvinylpirrolidone
PXRD	Powder X-ray Diffraction
SALE	Solvent Assisted Linker Exchange
SBU	Secondary Building Unit
SCXRD	Single-Crystal X-Ray Diffraction

SEM	Scanning Electron Microscopy
SIM	Solvothermal Deposition in Metal–Organic Frameworks
SOMC	Surface Organo-Metallic Chemistry
SSMS	Spark Source Mass Spectrometry
SS-NMR	Solid-State Nuclear Magnetic Resonance
TCPP	Tetrakis(4-carboxyphenyl) porphyrin
TEM	Transmission Electron Microscopy
TGA	Thermogravimetric Analysis
TIMS	Thermal Ionization-Mass Spectrometry
UNLPF	University of Nebraska-Lincoln Porous Framework
UV–Vis	Ultraviolet–Visible
XANES	X-Ray Absorption Near Edge Structure
XAS	X-Ray Absorption Spectroscopy
XPS	X-Ray Photoelectron Spectroscopy

References

1 Furukawa, H., Cordova, K.E., O'keeffe, M., and Yaghi, O.M. (2013). The chemistry and applications of metal-organic frameworks. *Science* 341: 1230444.

2 Zhou, S., Shekhah, O., Ramírez, A. et al. (2022). Asymmetric pore windows in MOF membranes for natural gas valorization. *Nature* 606: 706–712.

3 Liang, W., Xu, H., Carraro, F. et al. (2019). Enhanced activity of enzymes encapsulated in hydrophilic metal-organic frameworks. *J. Am. Chem. Soc.* 141 (6): 2348–2355.

4 Kim, E., Siegelman, R.L., Jiang, H.Z. et al. (2020). Cooperative carbon capture and steam regeneration with tetraamine-appended metal-organic frameworks. *Science* 369: 392–396.

5 Gascon, J., Corma, A., Kapteijn, F., and Llabrés I Xamena, F.X. (2014). Metal organic framework catalysis: quo vadis? *ACS Catal.* 4 (2): 361–378.

6 Bavykina, A., Kolobov, N., Khan, I.S. et al. (2020). Metal-organic frameworks in heterogeneous catalysis: recent progress, new trends, and future perspectives. *Chem. Rev.* 120 (16): 8468–8535.

7 McGuirk, C.M., Katz, M.K., Stern, C.L. et al. (2015). Turning on catalysis: Incorporation of a hydrogen-bond-donating squaramide moiety into a Zr metal-organic framework. *J. Am. Chem. Soc.* 137 (2): 919–925.

8 Corma, A., García, H., and Llabrés I Xamena, F.X. (2010). Engineering metal organic frameworks for heterogeneous catalysis. *Chem. Rev.* 110 (8): 4606–4655.

9 Yang, D., Babucci, M., Casey, W.H., and Gates, B.C. (2020). The surface chemistry of metal oxide qlusters: from metal-organic frameworks to minerals. *ACS Cent. Sci.* 6 (9): 1523–1533.

10 Trickett, C.A., Popp, T.M.O., Su, J. et al. (2019). Identification of the strong Brønsted acid site in a metal–organic framework solid acid catalyst. *Nat. Chem.* 11: 170–176.

11 Yoon, J.W., Seo, Y.-K., Hwang, Y.K. et al. (2010). Controlled reducibility of a metal-organic framework with coordinatively unsaturated sites for preferential gas sorption. *Angew. Chem. Int. Ed.* 49: 5949–5952.

12 Wei, Y.S., Zhang, M., Zou, R., and Xu, Q. (2020). Metal-organic framework-based catalysts with single metal sites. *Chem. Rev.* 120 (21): 12089–12174.

13 Vermoortele, F., Ameloot, A., Alaerts, L. et al. (2012). Tuning the catalytic performance of metal-organic frameworks in fine chemistry by active site engineering. *J. Mater. Chem.* 22: 10313–10321.

14 Ji, P., Feng, X., Oliveres, P. et al. (2019). Strongly Lewis acidic metal–organic frameworks for continuous flow catalysis. *J. Am. Chem. Soc.* 141 (37): 14878–14888.

15 Dhakshinamoorthy, A., Alvaro, M., Chevreau, H. et al. (2012). Iron(iii) metal-organic frameworks as solid Lewis acids for the isomerization of α-pinene oxide. *Catal. Sci. Technol.* 2: 324–330.

16 Alaerts, L., Séguin, E., Poelman, H. et al. (2006). Probing the lewis acidity and catalytic activity of the metal-organic framework $[Cu_3(btc)_2]$ (BTC = Benzene-1,3,5-tricarboxylate). *Chem. Eur. J.* 12: 7353–7363.

17 Nguyen, L.T.L., Nguyen, C.v., Dang, G.H. et al. (2011). Towards applications of metal-organic frameworks in catalysis: Friedel-Crafts acylation reaction over IRMOF-8 as an efficient heterogeneous catalyst. *J. Mol. Catal. A: Chem.* 349: 28–35.

18 Jiang, D., Mallat, T., Krumeich, F., and Baiker, A. (2008). Copper-based metal-organic framework for the facile ring-opening of epoxides. *J. Catal.* 257: 390–395.

19 Rojas-Buzo, S., Bohigues, B., Lopes, C.W. et al. (2021). Tailoring Lewis/Brønsted acid properties of MOF nodesviahydrothermal and solvothermal synthesis: simple approach with exceptional catalytic implications. *Chem. Sci.* 12: 10106–10115.

20 Zhai, Q.G., Bu, X., Mao, C. et al. (2016). Systematic and dramatic tuning on gas sorption performance in heterometallic metal-organic frameworks. *J. Am. Chem. Soc.* 138 (8): 2524–2527.

21 Syzgantseva, M.A., Ireland, C.P., Ebrahim, F.M. et al. (2019). Metal substitution as the method of modifying electronic structure of metal-organic frameworks. *J. Am. Chem. Soc.* 141 (15): 6271–6278.

22 Castells-Gil, J., Padial, N.M., Almora-Barrios, N. et al. (2018). Chemical engineering of photoactivity in heterometallic titanium–organic frameworks by metal doping. *Angew. Chem. Int. Ed.* 57: 8453–8457.

23 Gaillac, R., Pullumbi, P., Beyer, K.A. et al. (2017). Liquid metal–organic frameworks. *Nat. Mater.* 16: 1149–1155.

24 Terban, M.W. and Billinge, S.J.L. (2022). Structural analysis of molecular materials using the pair distribution function. *Chem. Rev.* 122 (1): 1208–1272.

25 Castillo-Blas, C., Moreno, J.M., Romero-Muñiz, I., and Platero-Prats, A.E. (2020). Applications of pair distribution function analyses to the emerging field of: non-ideal metal-organic framework materials. *Nanoscale* 12: 15577–15587.

26 Castells-Gil, J., Padial, N.M., Almora-Barrios, N. et al. (2020). Heterometallic titanium-organic frameworks as dual metal catalysts for synergistic non-buffered hydrolysis of nerve agent simulants. *Chem* 6 (11): 3118–3131.

27 Wang, L.J., Deng, H., Furukawa, H. et al. (2014). Synthesis and characterization of metal-organic framework-74 containing 2, 4, 6, 8 and 10 different metals. *Inorg. Chem.* 53 (12): 5881–5883.

28 Viciano-Chumillas, M., Liu, X., Leyva-Pérez, A. et al. (2022). Mixed component metal-organic frameworks: heterogeneity and complexity at the service of application performances. *Coord. Chem. Rev.* 451: 214273.

29 Syzgantseva, M.A., Ireland, C.P., Ebrahim, F.M. et al. (2019). Metal substitution as the method of modifying electronic structure of metal-organic frameworks. *J. Am. Chem. Soc.* 141 (15): 6271–6278.

30 Trousselet, F., Archereau, A., Boutin, A., and Coudert, F.X. (2016). Heterometallic metal-organic frameworks of MOF-5 and UiO-66 families: insight from computational chemistry. *J. Phys. Chem. C* 120 (43): 24885–24894.

31 Nouar, F., Devic, T., Chevreau, H. et al. (2012). Tuning the breathing behaviour of MIL-53 by cation mixing. *Chem. Commun.* 48: 10237–10239.

32 Depauw, H., Nevjestić, I., Wang, G. et al. (2017). Discovery of a novel, large pore phase in a bimetallic Al/V metal-organic framework. *J. Mater. Chem. A* 5: 24580–24584.

33 Horcajada, P., Surblé, S., Serre, C. et al. (2007). Synthesis and catalytic properties of MIL-100(Fe), an iron(III) carboxylate with large pores. *Chem. Commun.* 2820–2822.

34 Castells-Gil, J., Padial, N.M., Almora-Barrios, N. et al. (2019). Novo synthesis of mesoporous photoactive titanium(iv)-organic frameworks with MIL-100 topology. *Chem. Sci.* 10: 4313–4321.

35 Jia, H., Han, Q., Luo, W. et al. (2022). Sequence control of metals in MOF by coordination number precoding for electrocatalytic oxygen evolution. *Chem Catal.* 2 (84): 84–101.

36 Dissegna, S., Vervoorts, P., Hobday, C.L. et al. (2018). Tuning the mechanical response of metal-organic frameworks by defect engineering. *J. Am. Chem. Soc.* 140 (37): 11581–11584.

37 Shearer, G.C., Chavan, S., Bordiga, S. et al. (2016). Defect engineering: tuning the porosity and composition of the metal-organic framework UiO-66 via modulated synthesis. *Chem. Mater.* 28 (11): 3749–3761.

38 Wu, H., Chua, Y.S., Krungleviciute, V. et al. (2013). Unusual and highly tunable missing-linker defects in zirconium metal-organic framework UiO-66 and their important effects on gas adsorption. *J. Am. Chem. Soc.* 135 (28): 10525–10532.

39 Rodríguez-Albelo, L.M., López-Maya, E., Hamad, S. et al. (2017). Selective sulfur dioxide adsorption on crystal defect sites on an isoreticular metal organic framework series. *Nat. Commun.* 8: 14457.

40 Liu, Y., Klet, R.C., Hupp, J.T., and Farha, O. (2015). Probing the correlations between the defects in metal-organic frameworks and their catalytic activity by an epoxide ring-opening reaction. *Chem. Commun.* 52: 7806–7809.

41 Taddei, M. (2017). When defects turn into virtues: the curious case of zirconium-based metal-organic frameworks. *Coord. Chem. Rev.* 343: 1–24.

42 Feng, X., Jena, H.S., Krishnaraj, C. et al. (2021). Generating catalytic sites in UiO-66 through defect engineering. *ACS Appl. Mater. Interfaces* 13 (51): 60715–60735.

43 Lázaro, I.A., Almora-Barrios, N., Tatay, S., and Martí-Gastaldo, C. (2021). Effect of modulator connectivity on promoting defectivity in titanium-organic frameworks. *Chem. Sci.* 12: 2586–2593.

44 Gutov, O.v., Hevia, M.G., Escudero-Adán, E.C., and Shafir, A. (2015). Metal-organic framework (MOF) defects under control: insights into the missing linker sites and their implication in the reactivity of zirconium-based frameworks. *Inorg. Chem.* 54 (17): 8396–8400.

45 Valenzano, L., Civalleri, B., Chavan, S. et al. (2011). Disclosing the comp lex structure of UiO-66 metal organic framework: a synergic combination of experiment and theory. *Chem. Mater.* 23 (7): 1700–1718.

46 Ravon, U., Savonnet, M., Aguado, S. et al. (2010). Engineering of coordination polymers for shape selective alkylation of large aromatics and the role of defects. *Microporous Mesoporous Mater.* 129: 319–329.

47 Vermoortele, F., Bueken, B., Le Bars, G. et al. (2013). Synthesis modulation as a tool to increase the catalytic activity of metal-organic frameworks: the unique case of UiO-66(Zr). *J. Am. Chem. Soc.* 135 (31): 11465–11468.

48 Liu, L., Chen, Z., Wang, J. et al. (2019). Imaging defects and their evolution in a metal–organic framework at sub-unit-cell resolution. *Nat. Chem.* 11: 622–628.

49 Katz, M.J., Klet, R.C., Moon, S.-Y. et al. (2015). One step backward is two steps forward: enhancing the hydrolysis rate of UiO-66 by decreasing [OH-]. *ACS Catal.* 5 (8): 4637–4642.

50 Drake, T., Ji, P., and Lin, W. (2018). Site isolation in metal-organic frameworks enables novel transition metal catalysis. *Acc. Chem. Res.* 51 (9): 2129–2138.

51 Cui, X., Li, W., Ryabchuk, P. et al. (2018). Bridging homogeneous and heterogeneous catalysis by heterogeneous single-metal-site catalysts. *Nat. Catal.* 1: 385–397.

52 Gao, Z., Lai, Y., Gong, L. et al. (2022). Robust Th-MOF-supported semirigid single-metal-site catalyst for an efficient acidic oxygen evolution reaction. *ACS Catal.* 12 (15): 9101–9113.

53 Mandal, S., Natarajan, S., Mani, P., and Pankajakshan, A. (2021). Post-synthetic modification of metal–organic frameworks toward applications. *Adv. Funct. Mater.* 31 (4): 2006291.

54 Baranowski, C.J., Brandon, J., Bahmanpour, A.M., and Kröcher, O. (2021). Grafting of alkali metals on fumed silica for the catalytic dehydrogenation of methanol to formaldehyde. *ChemCatChem* 13 (17): 3864–3877.

55 Brozek, C.K. and Dincă, M. (2013). Ti^{3+}-, $V^{2+/3+}$-, $Cr^{2+/3+}$-, Mn^{2+}-, and Fe^{2+}-substituted MOF-5 and redox reactivity in Cr- and Fe-MOF-5. *J. Am. Chem. Soc.* 135 (34): 12886–12891.

56 Mondloch, J.E., Bury, W., Fairen-Jimenez, D. et al. (2013). Vapor-phase metalation by atomic layer deposition in a metal-organic framework. *J. Am. Chem. Soc.* 135 (28): 10294–10297.

57 Justin Kunene, T., Kwanda Tartibu, L., Ukoba, K., and Jen, T.C. (2022). Review of atomic layer deposition process, application and modeling tools. *Mater. Today Proc.* 62: S95–S109.

58 George, S.M. (2010). Atomic layer deposition: an overview. *Chem. Rev.* 110 (1): 111–131.

59 Yang, D., Odoh, S.O., Wang, T.C. et al. (2015). Metal-organic framework nodes as nearly ideal supports for molecular catalysts: NU-1000- and UiO-66-supported iridium complexes. *J. Am. Chem. Soc.* 137 (23): 7391–7396.

60 Noh, H., Cui, Y., Peters, A.W. et al. (2016). An exceptionally stable metal-organic framework supported molybdenum(VI) oxide catalyst for cyclohexene epoxidation. *J. Am. Chem. Soc.* 138 (44): 14720–14726.

61 Kim, I.S., Borycz, J., Platero-Prats, A.E. et al. (2015). Targeted single-site MOF node modification: trivalent metal loading via atomic layer deposition. *Chem. Mater.* 27 (13): 4772–4778.

62 Hackler, R.A., Pandharkar, R., Ferrandon, M.S.M. et al. (2020). Isomerization and selective hydrogenation of propyne: screening of metal-organic frameworks modified by atomic layer deposition. *J. Am. Chem. Soc.* 142 (48): 20380–20389.

63 Berijani, K., Morsali, A., and Hupp, J.T. (2019). An effective strategy for creating asymmetric MOFs for chirality induction: a chiral Zr-based MOF for enantioselective epoxidation. *Catal. Sci. Technol.* 9: 3388–3397.

64 Copéret, C., Comas-Vives, A., Conley, M.P. et al. (2016). Surface organometallic and coordination chemistry toward single-site heterogeneous catalysts: strategies, methods, structures, and activities. *Chem. Rev.* 116 (2): 323–421.

65 Samantaray, M.K., Pump, E., Bendjeriou-Sedjerari, A. et al. (2018). Surface organometallic chemistry in heterogeneous catalysis. *Chem. Soc. Rev.* 47: 8403–8437.

66 Basset, J.M. and Pelletier, J.D.A. (2018). Predictive approach of heterogeneous catalysis. *Natl. Sci. Rev.* 5: 633–635.

67 Manna, K., Ji, P., Greene, F.X., and Lin, W. (2016). Metal-organic framework nodes support single-site magnesium-alkyl catalysts for hydroboration and hydroamination reactions. *J. Am. Chem. Soc.* 138 (24): 7488–7491.

68 Thiam, Z., Abou-Hamad, E., Dereli, B. et al. (2020). Extension of surface organometallic chemistry to metal–organic frameworks: development of a well-defined single site $[(\equiv\mathrm{Zr}-\ \mathrm{O}-)\mathrm{W}(=\mathrm{O})(\mathrm{CH2}^{t}\mathrm{Bu})_3]$ olefin metathesis catalyst. *J. Am. Chem. Soc.* 142 (39): 16690–16703.

69 Yang, Q., Xu, Q., and Jiang, H.L. (2017). Metal–organic frameworks meet metal nanoparticles: synergistic effect for enhanced catalysis. *Chem. Soc. Rev.* 46 (15): 4774–4808.

70 Sui, J., Liu, H., Hu, S. et al. (2022). A general strategy to immobilize single-atom catalysts in metal–organic frameworks for enhanced photocatalysis. *Adv. Mater.* 34 (6): 2109203.

71 Du, Q., Rao, R., Bi, F. et al. (2022). Preparation of modified zirconium-based metal-organic frameworks (Zr-MOFs) supported metals and recent application in environment: a review and perspectives. *Surf. Interfaces* 28: 101647.

72 Zhuang, Z., Mai, Z., Wang, T., and Liu, D. (2020). Strategies for conversion between metal–organic frameworks and gels. *Coord. Chem. Rev.* 421: 213461.

73 Abednatanzi, S., Najafi, M., Gohari Derakhshandeh, P., and Van Der Voort, P. (2022). Metal- and covalent organic frameworks as catalyst for organic transformation: comparative overview and future perspectives. *Coord. Chem. Rev.* 451: 214259.

74 Wei, Y.-S., Zhang, M., Zou, R., and Xu, Q. (2020). Metal−organic framework-based catalysts with single metal sites. *Chem. Rev.* 120: 12089–12174.

75 Hwang, Y.K., Hong, D.-Y., Chang, J.-S. et al. (2008). Amine grafting on coordinatively unsaturated metal centers of MOFs: consequences for catalysis and metal encapsulation. *Angew. Chem.* 120 (22): 4212–4216.

76 Cohen, S.M., Zhang, Z., and Boissonnault, J.A. (2016). Toward "metallo-MOFzymes": metal-organic frameworks with single-site metal catalysts for small-molecule transformations. *Inorg. Chem.* 55 (15): 7281–7290.

77 Wen, Y., Zhang, J., Xu, Q. et al. (2018). Pore surface engineering of metal–organic frameworks for heterogeneous catalysis. *Coord. Chem. Rev.* 376: 248–276.

78 Yao, Y., Ma, Z., Dou, Y. et al. (2022). Random occupation of multimetal sites in transition metal-organic frameworks for boosting the oxygen evolution reaction. *Chem. A Eur. J.* 28 (14): e202104288.

79 Liberman, I., Shimoni, R., Ifraemov, R. et al. (2020). Active-site modulation in an Fe-porphyrin-based metal-organic framework through ligand axial coordination: accelerating electrocatalysis and charge-transport kinetics. *J. Am. Chem. Soc.* 142 (4): 1933–1940.

80 Song, F., Zhang, T., Wang, C., and Lin, W. (2012). Chiral porous metal-organic frameworks with dual active sites for sequential asymmetric catalysis. *Proc. R Soc.* 468 (2143): 2035–2052.

81 Isaeva, V.I. and Kustov, L.M. (2010). The application of metal-organic frameworks in catalysis (review). *Pet. Chem.* 50 (3): 167–180.

82 Li, D., Xu, H.Q., Jiao, L., and Jiang, H.L. (2019). Metal-organic frameworks for catalysis: state of the art, challenges, and opportunities. *EnergyChem* 1 (1): 100005.

83 Wu, C.-D., Zhao, M., Wu, C.-D., and Zhao, M. (2017). Incorporation of molecular catalysts in metal–organic frameworks for highly efficient heterogeneous catalysis. *Adv. Mater.* 29 (14): 1605446.

84 Tu, W., Xu, Y., Yin, S., and Xu, R. (2018). Rational design of catalytic centers in crystalline frameworks. *Adv. Mater.* 30 (33): 1707582.

85 Shi, K., Lin, Y., Xiong, Z. et al. (2022). Synergistic effects of porphyrin-ring catalytic center and metal catalytic site from crosslinked porphyrin-based porous polyimides cathode host for lithium polysulfides conversion in lithium-sulfur batteries. *Chem. Eng. J.* 430: 132692.

86 Manna, K., Zhang, T., and Lin, W. (2014). Postsynthetic metalation of bipyridyl-containing metal-organic frameworks for highly efficient catalytic organic transformations. *J. Am. Chem. Soc.* 136 (18): 6566–6569.

87 Ranjan Jena, S., Mandal, T., and Choudhury, J. (2022). Metal-terpyridine assembled functional materials for electrochromic, catalytic and environmental applications. *Chem. Rec.* 22 (12): e202200165.

88 Chen, L., Jiang, Y., Huo, H. et al. (2020). Metal-organic framework-based composite Ni@MOF as heterogenous catalyst for ethylene trimerization. *Appl. Catal., A* (594): 117457.

89 Xu, Z., Shen, J., Li, L. et al. (2022). (Salen)Titanium-catalyzed asymmetric hydrogen atom transfer for epoxides reduction. *Angew. Chem.* 61 (50): e202214111.

90 Drake, T., Ji, P., and Lin, W. (2018). Site isolation in metal-organic frameworks enables novel transition metal catalysis. *Acc. Chem. Res.* 51 (9): 2129–2138.

91 Ma, L., Abney, C., and Lin, W. (2009). Enantioselective catalysis with homochiral metal–organic frameworks. *Chem. Soc. Rev.* 38 (5): 1248–1256.

92 Senge, M.O., Sergeeva, N.N., and Hale, K.J. (2021). Classic highlights in porphyrin and porphyrinoid total synthesis and biosynthesis. *Chem. Soc. Rev.* 50 (7): 4730–4789.

93 Barona-Castaño, J.C., Carmona-Vargas, C.C., Brocksom, T.J. et al. (2016). Porphyrins as catalysts in scalable organic reactions. *Molecules* 21, 21 (3): 310.

94 Usov, P.M., Ahrenholtz, S.R., Maza, W.A. et al. (2016). Cooperative electrochemical water oxidation by Zr nodes and Ni–porphyrin linkers of a PCN-224 MOF thin film. *J. Mater. Chem. A* 4 (43): 16818–16823.

95 Shultz, A.M., Farha, O.K., Hupp, J.T., and Nguyen, S.T. (2009). A catalytically active, permanently microporous MOF with metalloporphyrin struts. *J. Am. Chem. Soc.* 131 (12): 4204–4205.

96 Fateeva, A., Chater, P.A., Ireland, C.P. et al. (2012). A water-stable porphyrin-based metal–organic framework active for visible-light photocatalysis. *Angew. Chem. Int. Ed.* 51 (30): 7440–7444.

97 Bai, Y., Dou, Y., Xie, L.H. et al. (2016). Zr-based metal–organic frameworks: design, synthesis, structure, and applications. *Chem. Soc. Rev.* 45 (8): 2327–2367.

98 Feng, D., Gu, Z.Y., Li, J.R. et al. (2012). Zirconium-metalloporphyrin PCN-222: mesoporous metal-organic frameworks with ultrahigh stability as biomimetic catalysts. *Angew. Chem. Int. Ed.* 51 (41): 10307–10310.

99 Jiang, H.L., Feng, D., Wang, K. et al. (2013). An exceptionally stable, porphyrinic Zr metal-organic framework exhibiting pH-dependent fluorescence. *J. Am. Chem. Soc.* 135 (37): 13934–13938.

100 Huang, N., Wang, K., Drake, H. et al. (2018). Tailor-made pyrazolide-based metal-organic frameworks for selective catalysis. *J. Am. Chem. Soc.* 140 (20): 6383–6390.

101 Ishimizu, Y., Ma, Z., Hada, M., and Fujii, H. (2021). Rate-limiting step of epoxidation reaction of the oxoiron(IV) porphyrin π-cation radical complex: electron transfer coupled bond formation mechanism. *Inorg. Chem.* 60: 17687–17698.

102 Nakagaki, S., Ferreira, G.K.B., Ucoski, G.M., and KAD, d.F.C. (2013). Chemical reactions catalyzed by metalloporphyrin-based metal-organic frameworks. *Molecules* 18: 7279–7308.

103 Hod, I., Sampson, M.D., Deria, P. et al. (2015). Fe-porphyrin-based metal-organic framework films as high-surface concentration, heterogeneous catalysts for electrochemical reduction of CO_2. *ACS Catal.* 5 (11): 6302–6309.

104 Bipyridine. (2006) Wikipedia. https://en.wikipedia.org/wiki/Bipyridine.

105 Canivet, J., Aguado, S., Schuurman, Y., and Farrusseng, D. (2013). MOF-supported selective ethylene dimerization single-site catalysts through one-pot postsynthetic modification. *J. Am. Chem. Soc.* 135 (11): 4195–4198.

106 Song, F., Wang, C., Falkowski, J.M. et al. (2010). Isoreticular chiral metal-organic frameworks for asymmetric alkene epoxidation: tuning catalytic activity by controlling framework catenation and varying open channel sizes. *J. Am. Chem. Soc.* 132 (43): 15390–15398.

107 Shimizu, S., Watanabe, N., Kataoka, T. et al. (2012). Pyridine and pyridine derivatives. *Ullmann's Encycl. Ind. Chem.* 30: 557–586.

108 Wang, C., Xie, Z., Dekrafft, K.E., and Lin, W. (2011). Doping metal-organic frameworks for water oxidation, carbon dioxide reduction, and organic photocatalysis. *J. Am. Chem. Soc.* 133 (34): 13445–13454.

109 Hou, C.C., Li, T.T., Cao, S. et al. (2015). Incorporation of a [Ru(dcbpy)(bpy) 2] 2+ photosensitizer and a Pt(dcbpy)Cl 2 catalyst into metal–organic frameworks for photocatalytic hydrogen evolution from aqueous solution. *J. Mater. Chem. A* 3 (19): 10386–10394.

110 Chen, G.H., Leu, W.J., Guh, J.H. et al. (2018). Synthesis, characterization and cancer cell growth inhibition activity of ruthenium(II) complexes bearing bidentate pyrrole-imine ligands. *J. Organomet. Chem.* 868: 122–130.

111 Jin, Y., Zhu, Y., and Zhang, W. (2013). Development of organic porous materials through Schiff-base chemistry. *CrystEngComm* 15 (8): 1484–1499.

112 Schenkel, L.B. and Ellman, J.A. (2003). Novel sulfinyl imine ligands for asymmetric catalysis. *Org. Lett.* 5 (4): 545–548.

113 Cozzi, P.G. (2004). Metal–Salen Schiff base complexes in catalysis: practical aspects. *Chem. Soc. Rev.* 33 (7): 410–421.

114 Kitaura, R., Onoyama, G., Sakamoto, H. et al. (2004). Immobilization of a metallo schiff base into a microporous coordination polymer. *Angew. Chem. Int. Ed.* 43 (20): 2684–2687.

115 Yuan, G., Jiang, H., Zhang, L. et al. (2019). Metallosalen-based crystalline porous materials: synthesis and property. *Coord. Chem. Rev.* (378): 483–499.

116 Li, C., Ma, Z., Li, S. et al. (2018). Syntheses, structures and catalytic activities of molybdenum carbonyl complexes based on pyridine-imine ligands. *Transition Met. Chem.* 43 (2): 193–199.

117 Yoon, M., Srirambalaji, R., and Kim, K. (2012). Homochiral metal-organic frameworks for asymmetric heterogeneous catalysis. *Chem. Rev.* 112 (2): 1196–1231.

118 Su, D.S., Zhang, J., Frank, B. et al. (2010). Metal-free heterogeneous catalysis for sustainable chemistry. *ChemSusChem* 3 (2): 169–180.

119 Palucki, M., Finney, N.S., Pospisil, P.J. et al. (1998). The mechanistic basis for electronic effects on enantioselectivity in the (salen)Mn(III)-catalyzed epoxidation reaction. *J. Am. Chem. Soc.* 120 (5): 948–954.

120 Phan, N.T.S., Nguyen, C.K., Nguyen, T.T., and Truong, T. (2014). Towards applications of metal–organic frameworks in catalysis: C–H direct activation of benzoxazole with aryl boronic acids using Ni 2 (BDC) 2 (DABCO) as an efficient heterogeneous catalyst. *Catal. Sci. Technol.* 4 (2): 369–377.

121 Chughtai, A.H., Ahmad, N., Younus, H.A. et al. (2015). Metal–organic frameworks: versatile heterogeneous catalysts for efficient catalytic organic transformations. *Chem. Soc. Rev.* 44 (19): 6804–6849.

122 Wei, Y.S., Zhang, M., Zou, R., and Xu, Q. (2020). Metal-organic framework-based catalysts with single metal sites. *Chem. Rev.* 120 (21): 12089–12174.

123 Mackay, L.G., Stephen Wylie, R., Sanders, M., and JK. (1994). Catalytic acyl transfer by a cyclic porphyrin trimer: efficient turnover without product inhibition. *J. Am. Chem. Soc.* 116 (4): 8980.

124 Huang, Y.B., Liang, J., Wang, X.S., and Cao, R. (2017). Multifunctional metal–organic framework catalysts: synergistic catalysis and tandem reactions. *Chem. Soc. Rev.* 46 (1): 126–157.

125 Chakrabarty, R., Mukherjee, P.S., and Stang, P.J. (2011). Supramolecular coordination: Self-assembly of finite two- and three-dimensional ensembles. *Chem. Rev.* 111 (11): 6810–6918.

126 Yang, X.L., Xie, M.H., Zou, C. et al. (2012). Porous metalloporphyrinic frameworks constructed from metal 5,10,15,20-tetrakis(3,5-biscarboxylphenyl) porphyrin for highly efficient and selective catalytic oxidation of alkylbenzenes. *J. Am. Chem. Soc.* 134 (25): 10638–10645.

127 Grützmacher, H. (2008). Cooperating ligands in catalysis. *Angew. Chem. Int. Ed.* 47 (10): 1814–1818.

128 Walter, C.J., Anderson, H.L., and Sanders, J.K.M. (1993). exo -Selective acceleration of an intermolecular Diels–Alder reaction by a trimeric porphyrin host. *J. Chem. Soc., Chem. Commun.* 0 (5): 458–460.

129 Berrisford, D.J., Bolm, C., and Sharpless, K.B. (1995). Ligand-accelerated catalysis. *Angew. Chem. Int. Ed.* 34 (10): 1059–1070.

130 Jacobsen, E.N., Markó, I., Mungall, W.S. et al. (1988). Asymmetric dihydroxylation via ligand-accelerated catalysis. *J. Am. Chem. Soc.* 110 (6): 1968–1970.

131 Carson, F., Martínez-Castro, E., Marcos, R. et al. (2015). Effect of the functionalisation route on a Zr-MOF with an Ir–NHC complex for catalysis. *Chem. Commun.* 51 (54): 10864–10867.

132 Song, L.F., Jiang, C.H., Jiao, C.L. et al. (2010). Two new metal-organic frameworks with mixed ligands of carboxylate and bipyridine: synthesis, crystal structure, and sensing for methanol. *Cryst Growth Des.* 10 (12): 5020–5023.

133 Masoomi, M.Y., Morsali, A., Dhakshinamoorthy, A., and Garcia, H. (2019). Mixed-metal MOFs: unique opportunities in metal-organic framework functionality and design. *Angew. Chem. Int. Ed. Engl.* 141 (43): 15330–15347.

134 Wang, C., Wang, J.L., and Lin, W. (2012). Elucidating molecular iridium water oxidation catalysts using metal-organic frameworks: a comprehensive structural, catalytic, spectroscopic, and kinetic study. *J. Am. Chem. Soc.* 134 (48): 19895–19908.

135 Xie, M.H., Yang, X.L., Zou, C., and De, W.C. (2011). A SnIV-porphyrin-based metal-organic framework for the selective photo-oxygenation of phenol and sulfides. *Inorg. Chem.* 50 (12): 5318–5320.

136 Zhao, M., Ou, S., and De, W.C. (2014). Porous metal-organic frameworks for heterogeneous biomimetic catalysis. *Acc. Chem. Res.* 47 (4): 1199–1207.

137 Taddei, M., Wakeham, R.J., Koutsianos, A. et al. (2018). Post-synthetic ligand exchange in zirconium-based metal-organic frameworks: beware of the defects! *Angew. Chemie.* 130 (36): 11880–11884.

138 Hoffmann, H.C., Debowski, M., Müller, P. et al. (2012). Solid-state NMR spectroscopy of metal–organic framework compounds (MOFs). *Materials* 5: 2537–2572.

139 Kim, M., Cahill, J.F., Fei, H. et al. (2012). Postsynthetic ligand and cation exchange in robust metal-organic frameworks. *J. Am. Chem. Soc.* 134 (43): 18082–18088.

140 Yu, X. and Cohen, S.M. (2016). Photocatalytic metal-organic frameworks for selective 2,2,2-trifluoroethylation of styrenes. *J. Am. Chem. Soc.* 138 (38): 12320–12323.

141 Roy, S., Bhunia, A., Schuth, N. et al. (2018). Light-driven hydrogen evolution catalyzed by a cobaloxime catalyst incorporated in a MIL-101(Cr) metal–organic framework. *Sustainable Energy Fuels* 2 (6): 1148–1152.

142 García-Simón, C., Gramage-Doria, R., Raoufmoghaddam, S. et al. (2015). Enantioselective hydroformylation by a Rh-catalyst entrapped in a supramolecular metallocage. *J. Am. Chem. Soc.* 137 (7): 2680–2687.

143 Bhunia, A., Johnson, B.A., Czapla-Masztafiak, J. et al. (2018). Formal water oxidation turnover frequencies from MIL-101(Cr) anchored Ru(bda) depend on oxidant concentration. *Chem. Commun.* 54 (56): 7770–7773.

144 Li, B., Zhang, Y., Ma, D. et al. (2012). A strategy toward constructing a bifunctionalized MOF catalyst : post-synthetic modification of MOFs on organic ligands and coordinatively unsaturated metal sites. *Chem. Commun.* 48 (49): 6151–6153.

145 Maza, W.A. and Morris, A.J. (2014). Photophysical characterization of a ruthenium(II) tris(2,2′- bipyridine)-doped zirconium UiO-67 metal-organic framework. *J. Phys. Chem. C* 118 (17): 8803–8817.

146 Pullen, S., Roy, S., and Ott, S. (2017). [FeFe] Hydrogenase active site model chemistry in a UiO-66 metal–organic framework. *Chem. Commun.* 53 (37): 5227–5230.

147 Kajiwara, T., Fujii, M., Tsujimoto, M. et al. (2016). Photochemical reduction of low concentrations of CO_2 in a porous coordination polymer with a ruthenium(II)–CO complex. *Angew. Chem. Int. Ed.* 55 (8): 2697–2700.

148 Shearer, G.C., Vitillo, J.G., Bordiga, S. et al. (2016). Functionalizing the defects: postsynthetic ligand exchange in the metal organic framework UiO-66. *Chem. Mater.* 28 (20): 7190–7193.

149 Karagiaridi, O., Bury, W., Mondloch, J.E. et al. (2014). Solvent-assisted linker exchange: an alternative to the De Novo synthesis of unattainable metal–organic frameworks. *Angew. Chem. Int. Ed.* 53 (18): 4530–4540.

150 Evans, J.D., Sumby, C.J., and Doonan, C.J. (2014). Post-synthetic metalation of metal–organic frameworks. *Chem. Soc. Rev.* 43 (16): 5933–5951.

151 Zhao, W., Li, G., and Tang, Z. (2019). Metal-organic frameworks as emerging platform for supporting isolated single-site catalysts. *Nano Today* 27: 178–197.

152 Gao, W.Y., Chrzanowski, M., and Ma, S. (2014). Metal–metalloporphyrin frameworks: a resurging class of functional materials. *Chem. Soc. Rev.* 43 (16): 5841–5866.

153 Luo, S., Li, X., Gao, W. et al. (2019). An MOF-derived C@NiO@Ni electrocatalyst for N2 conversion to NH3 in alkaline electrolytes. *Sustainable Energy Fuels* 4 (1): 164–170.

154 Wu, S., Chen, L., Yin, B., and Li, Y. (2015). “Click” post-functionalization of a metal–organic framework for engineering active single-site heterogeneous Ru(III) catalysts. *Chem. Commun.* 51 (48): 9884–9887.

155 Mon, M., Ferrando-Soria, J., Grancha, T. et al. (2016). Selective gold recovery and catalysis in a highly flexible methionine-decorated metal-organic framework. *J. Am. Chem. Soc.* 138 (25): 7864–7867.

156 Mon, M., Rivero-Crespo, M.A., Esfflsf Errando-Soria, J. et al. (2018). Synthesis of densely packaged, ultrasmall Pt02 clusters within a thioether-functionalized MOF: catalytic activity in industrial reactions at low temperature. *Angew. Chem.* 130 (21): 6294–6299.

157 Shi, W., Cao, L., Zhang, H. et al. (2017). surface modification of two-dimensional metal–organic layers creates biomimetic catalytic microenvironments for selective oxidation. *Angew. Chem.* 129 (33): 9836–9841.

158 Zuo, Q., Tingting Liu, T., Chen, C. et al. (2019). Ultrathin metal–organic framework nanosheets with ultrahigh loading of single Pt atoms for efficient visible-light-driven photocatalytic H2 evolution. *Angew. Chem. Int. Ed.* 58 (30): 10198–10203.

159 Tanabe, K.K. and Cohen, S.M. (2009). Engineering a metal–organic framework catalyst by using postsynthetic modification. *Angew. Chem.* 121 (40): 7560–7563.

160 Al-Attas, T.A., Marei, N.N., Yong, X. et al. (2021). Ligand-engineered metal-organic frameworks for electrochemical reduction of carbon dioxide to carbon monoxide. *ACS Catal.* 11 (12): 7350–7357.

161 Boissonnault, J.A., Wong-Foy, A.G., and Matzger, A.J. (2017). Core-shell structures arise naturally during ligand exchange in metal-organic frameworks. *J. Am. Chem. Soc.* 139 (42): 14841–14844.

162 Becker, W. (2012). Fluorescence lifetime imaging – techniques and applications. *J. Microsc.* 247 (2): 119–136.

163 Schrimpf, W., Jiang, J., Ji, Z. et al. (2018). Chemical diversity in a metal–organic framework revealed by fluorescence lifetime imaging. *Nat. Commun.* 9 (1): 1–10.

164 dos Santos, A.C.V.D., Lendl, B., and Ramer, G. (2022). Systematic analysis and nanoscale chemical imaging of polymers using photothermal-induced resonance (AFM-IR) infrared spectroscopy. *Polym. Test.* 106: 107443.

165 Thacker, N.C., Lin, Z., Zhang, T. et al. (2016). Robust and porous β-diketiminate-functionalized metal-organic frameworks for earth-abundant-metal-catalyzed C-H amination and hydrogenation. *J. Am. Chem. Soc.* 138 (10): 3501–3509.

166 He, C., Liang, J., Zou, Y.H. et al. (2022). Metal-organic frameworks bonded with metal N-heterocyclic carbenes for efficient catalysis. *Natl. Sci. Rev.* 9 (6).

167 Sing, K.S.W., Everett, D.H., Haul, R.A.W. et al. (1985). Reporting physisorption data for gas/solid systems with special reference to the determination of surface area and porosity. *Pure Appl. Chem.* 57 (4): 603–619.

168 Rouquerol, J., Avnir, D., Fairbridge, C.W. et al. (1994). Recommendations for the characterization of porous solids. *Pure Appl. Chem.* 66 (8): 1739–1758.

169 Thommes, M., Kaneko, K., Nimark, A.V. et al. (2015). Physisorption of gases, with special reference to the evaluation of Surface area and pore size distribution. *Pure Appl. Chem.* 87 (9–10): 1051–1069.

170 Farha, O.K., Zhang, X., Chen, Z. et al. (2020). A historical overview of activation and porosity of metal-organic frameworks. *Chem. Soc. Rev.* 49: 7406–7427.

171 Suendo, V., Nurhayati, Alni, A. et al. (2020). Revealing the real size of a porphyrin molecule with quantum confinement probing via temperature-dependent photoluminescence spectroscopy. *J. Phys. Chem. A* 124 (13): 2672–2682.

172 Xiang, W., Zhang, Y., Lin, H., and Liu, C. (2017). Nanoparticles/metal-organic framework composites for catalytic applications: current status and perspective. *Molecules* 22 (12): 2103–2036.

173 Farha, O.K. and Buru, C.T. (2020). Strategies for incorporating catalytically active polyoxometalates in metal-organic frameworks for organic transformations. *ACS Appl. Mater. Interfaces* 12 (5): 5345–5360.

174 Sun, J., Abednatanzi, S., Van Der Voort, P. et al. (2020). POM@MOF hybrids: synthesis and applications. *Catalysts* 10 (5): 578–608.

175 Farha, O.K., Hupp, J.T., Liu, J. et al. (2022). MOF-enabled confinement and related effects for chemical catalyst presentation and utilization. *Chem. Soc. Rev.* 51: 1045–1097.

176 Férey, G., Mellot-Drazmieks, C., Serre, C. et al. (2005). A chromium terephthalate-based solid with unusually large pore volumes and surface area. *Science* 309 (5743): 2040–2042.

177 Maksimchuk, N.V., Timofeeva, M.N., Melgunov, M.S. et al. (2008). Heterogeneous selective oxidation catalysts based on coordination polymer MIL-101 and transition metal-substituted polyoxometalates. *J. Catal.* 257 (2): 315–323.

178 Sabo, M., Henschel, A., Fröde, H. et al. (2007). Solution infiltration of palladium into MOF-5: synthesis, physisorption and catalytic properties. *J. Mater. Chem.* 17: 3827–3832.

179 Esken, D., Zhang, X., Lebedev, O.I. et al. (2009). Pd@MOF-5: limitations of gas-phase infiltration and solution impregnation of $[Zn_4O(bdc)_3]$ (MOF-5) with metal-organic palladium precursors for loading with Pd nanoparticles. *J. Mater. Chem.* 19: 1314–1319.

180 Kuang, Q., Chen, L., Zhang, X. et al. (2020). The function of metal-organic frameworks in the application of MOF-based composites. *Nanoscale Adv.* 2: 2628–2647.

181 Xu, Q., Aijaz, A., Karkamkar, A. et al. (2012). Immobilizing highly catalytically active Pt nanoparticles inside the pores of metal-organic framework: a double solvents approach. *J. Am. Chem. Soc.* 134 (34): 13926–13929.

182 Hermes, S., Schröder, F., Amirjalayer, S. et al. (2006). Loading of porous metal-organic open frameworks with organometallic CVD precursors: inclusion compounds of the type $[L_nM]_a$@MOF-5. *J. Mater. Chem.* 16: 2464–2472.

183 Okumura, M., Tanaka, K., Ueda, A., and Haruta, M. (1997). The reactivities of dimethylgold (III) β-diketone on the surface of TiO_2: a novel preparation method for Au catalysts. *Solid State Ionics* 95 (1–2): 143–149.

184 Okumura, M., Tsubota, S., Iwamoto, M., and Haruta, M. (1998). Chemical vapor deposition of gold nanoparticles on MCM-41 and their catalytic activities for the low-temperature oxidation of CO and of H_2. *Chem. Lett.* 27 (4): 315–316.

185 Hermes, S., Schröter, M.-K., Schmid, R. et al. (2005). Metal@MOF: loading of highly porous coordination polymers host lattices by metal organic chemical vapor deposition. *Angew. Chem. Int. Ed.* 44 (38): 6237–6241.

186 Hermannsdörfer, J., Friedrich, M., Miyajima, N. et al. (2012). Ni/Pd@MIL-101: synergistic catalysis with cavity-conform Ni/Pd nanoparticles. *Angew. Chem. Int. Ed.* 51 (46): 11473–11477.

187 Schröder, F., Esken, D., Cokoja, M. et al. (2008). Ruthenium nanoparticles inside porous $[Z_{n4}O(bdc)_3]$ by hydrogenolysis of adsorbed [Ru(cod)(cot)]: a solid-state reference system for surfactant-stabilized ruthenium colloids. *J. Am. Chem. Soc.* 130 (19): 6119–6130.

188 Li, B., Zhang, Y., Ma, D. et al. (2014). Metal-cation-directed *de Novo* assembly of a functionalized guest molecule in the nanospace of a metal-organic framework. *J. Am. Chem. Soc.* 136 (4): 1202–1205.

189 An, J., Geib, S.J., and Rosi, N.L. (2009). Cation-triggered drug release from porous zin-adeninate metal-organic framework. *J. Am. Chem. Soc.* 131 (24): 8376–8377.

190 Feng, D., Liu, T.F., Su, J. et al. (2015). Stable metal-organic frameworks containing single-molecule traps for enzyme encapsulation. *Nat. Commun.* 6: 5979–5986.

191 Chen, L., Zhang, X., Cheng, X. et al. (2020). The function of metal-organic frameworks in the application of MOF-based composites. *Nanoscale Adv.* 2: 2628–2647.

192 Larsen, R.W., Wojtas, L., Perman, J. et al. (2011). Mimicking heme enzymes in the solid state: metal-organic materials with selectively encapsulated heme. *J. Am. Chem. Soc.* 133 (27): 13056–10359.

193 Sun, W.Y., Liu, Z.Q., Yan, T., and Guo, J.H. (2021). Metalloporphyrin encapsulation for enhanced conversion of CO_2 to C_2H_4. *ACS Appl. Mater. Interfaces* 13 (22): 25937–25945.

194 Lu, G., Li, S., Guo, Z. et al. (2012). Imparting functionality to a metal-organic framework material by controlled nanoparticles encapsulation. *Nat. Chem.* 4: 310–316.

195 Opelt, S., Turk, S., Dietzsch, E. et al. (2008). Preparation of palladium supported on MOF-5 and its use as hydrogenation catalyst. *Catal. Commun.* 9 (6): 1286–1290.

196 Huang, L., Wang, H., Chen, J. et al. (2003). Synthesis, morphology control and properties of porous metal-organic coordination polymers. *Microporous Mesoporous Mater.* 58 (2): 105–114.